`

The Role of Whole Bone Marrow Cells in Scar Formation after Reperfusion of Myocardial Infarction in a Mouse Model

Inaugural-Dissertation
zur Erlangung des Doktorgrades
der Hohen Medizinischen Fakultät
der Rheinischen Friedrich-Wilhelms-Universität
Bonn

Naziha Hamad M Elhafi

aus Benghazi / Libya

2013

Angefertigt mit Genehmigung der
Medizinischen Fakultät der Universität Bonn

1. Gutachter: Prof. Dr. med Bernd Fleischmann
2. Gutachter: Prof. Dr. R. Meyer

Tag der Mündlichen Prüfung: 21.03.2013

Aus dem Institut für Physiologie I
Rheinische Friedrich-Wilhelms-Universität Bonn
Direktor: Prof. Dr. med. Bernd K. Fleischmann

I dedicate my thesis to my loving parents, to my dear husband and my kinder

Table of contents

List of abbreviations

BM	Bone Marrow
BMMNC	Bone Marrow MonoNuclear Cell
BMSCs	Bone Marrow Stem Cells
CG	Control Group
CAD	Coronary Artery Disease
CCM	Cellular Cardio Myoplasty
cDNA	copy Desoxyrib Nucleic Acid
CVD	Cardio Vascular Disease
CHD	Coronary Heart Disease
CXCR3	CXC- Chemokine Receptor-3
DAB	Diaminobenzidine
DEPC	Diethylpyrocarbonate
DNA	DesoxyriboNucleic Acid
ECG	Electrocardiogram
ECM	Extra Cellular Matrix
EGFP	Enhanced Green Fluorescent Protein
EF	Ejection Fraction
EPC	Endothelial progenitor cells
FGF	Fibroblast Growth Factor
GAPDH	Glycero Adehyd-3-Phosphate Dehydrogenase
GTP	Guanosine Tri Phosphate
H/E	Haematoxylin /Eosin
H_2O_2	Hydrogen peroxide
HR	Heart Rate
HSC	Haematopoietic Stem Cell
ICAM-1	Intra Cellular Adhesion Molecule 1
I.V	Intravenous
I/R	Ischemia and Reperfusion
IL	Interleukin
KO	Knockout mice

LAD	Left Anterior Descending
LPS	Lipo Poly Saccharide
LV	Left Ventricle
LVEDV	Left Ventricular End Diastolic Volume
LVsyst	Left Ventricle systolic
LVESP	Left Ventricle End Systole Pressure
MCP-1	Monocyte Chemoattractant Protein-1
MI	Myocardial Infarction
MIP	Macrophage Inflammatory Protein
MMP	Matrix MetalloProteinase
mRNA	messenger-RiboNucleic Acide
MSC	Mesenchymal Stem Cell
MOM	Mouse On Mouse
NTC	Non Template Control
OP	Operation
PBS	Phosphate Buffer Solution
PCR	Polymerase Chain Reaction
RNA	RiboNucleic Acid
RNase	RiboNuklease
RT-PCR	Real Time Polymerase Chain Reaction
TIMP	Tissue Inhibitor of Metalloproteinases
VEGF	Vascular Endotheial Growth Factor
WT	Wildtype
WBM	Whole Bone Marrow
α-SMAc	alpha-Smooth Muscle Actin

Zusammenfassung

Koronare Herzkrankheit und Myokardinfarkt sind assoziiert mit signifikanter Morbidität und Mortalität. Eine frühe Reperfusion des Myokardinfarkts wird therapeutisch angestrebt, aber der nachfolgende Gewebeumbau geht mit einer hohen Komplikationsrate einher. Unter innovativen therapeutischen Ansätzen wurde in den letzten Jahren die Zellersatztherapie erprobt, die über einen verbesserten Gewebeumbau und eine verminderte Narbengröße Verbesserungen im Langzeitüberleben und Funktion zu erzielen versucht. Wir untersuchten daher die Rolle von i.v. verabreichten Knochenmarkszellen nach Myokardinfarkt in einem Mausmodel. Die Herzen wurden funktionell untersucht und für histologische und morphometrische Auswertung sowie mRNA-Expressionsmessungen (RT-PCR) verarbeitet.

Kontrollmäuse bekamen PBS injiziert und zeigten eine rasche Entwicklung einer stabilen Myokardnarbe nach 7 Tagen Reperfusion, die bis nach 28 Tagen unverändert blieb. Injektion von Knochenmarkszellen unmittelbar nach Reperfusion führte zur signifikant besseren Pumpfunktion und geringerer Narbengröße nach 28 Tagen Reperfusion. Injektion von Knochenmarkszellen nach 3 Tagen Reperfusion zeigte eine tendentielle Verbesserung der Pumpfunktion und eine signifikant kleinere Narbe nach 28 Tagen, während beide Gruppen auch eine höhere Anzahl von Arteriolen in der Narbe aufwiesen. Die Auswertung der zellulären Mechanismen ergab eine verlängerte Entzündungsreaktion mit vorwiegender Beteiligung von Makrophagen, die insbesondere nach i.v. Gabe von Knochenmarkszellen nach 3 Tagen Reperfusion zu einem verzögerten Gewebeumbau mit Persistenz der Myofibroblasten in der Narbe führte. Die bessere Pumpfunktion nach Zellinjektion könnte mit aktivem Gewebeumbau nach 28 Tagen Reperfusion zusammen hängen, da hier Makrophagen in der Narbe persistierten. Weitere Auswertungen legten eine Rezirkulation der injizierten Zellen aus der Milz nahe, die sich möglicherweise in Makrophagen differenzieren. Im Gegensatz zu den Kontrolltieren führten die Knochenmarkszellen zu einer proinflammatorischen Aktivität von Zytokinen und Chemokinen nach 7 Tagen Reperfusion, während gleichzeitig die Marker des Gewebeumbaus eine verzögerte Narbenbildung zeigten.

Zusammenfassend führte Knochenmarkszellinjektion nach Reperfusion des Myokardinfarktes zur funktionellen Verbesserung aufgrund des persistierenden Gewebeumbaus und günstigen Lokalbedingungen der proinflammatorischen Reaktion. Die sofortige Zellinjektion zeigte eine bessere Pumpfunktion als die Injektion nach 3 Tagen Reperfusion. Diese Ergebnisse und das

Verständnis der Pathomechanismen sollen in weiteren Studien überprüft und vertieft werden, um das Potential für künftige klinische Anwendung zu untersuchen.

1 Introduction

1.1 Coronary Artery Disease

Coronary artery disease (CAD), syn. ischemic heart disease, is one of the major entities of all cardiovascular diseases and is associated with high morbidity and mortality. In 2002 the World Health Organization estimated that 12.6 % of deaths worldwide were attributable to ischemic heart disease. Despite significant improvements in treatment, CAD still affects approx 15.8 million people in the U.S.A (Rosamond et al., 2007).

CAD is a condition in which the blood flow through the coronary artery does not meet the substrate demand in myocardium. The myocardium becomes hypoxic and patients may report symptoms of angina pectoris. There are several risk factors for CAD to include: hypertension, diabetes, hyperlipidemia and family history. CAD is associated with metabolic syndrome, which is a cluster of cardiovascular disease risk factors whose underlying pathophysiology is supposedly related to insulin resistance. Metabolic syndrome affects one in five people, while some studies estimate that prevalence in the USA is as much as 25 % (Ford et al., 2002). A clinical episode of angina pectoris is usually a reversible situation where ischemic episodes cease within a short period of time. However, after a prolonged duration of ischemic episode, the myocardium suffers irreversible damage thereby leading to Myocardial Infarction (MI).
MI develops after a coronary vessel occlusion persists for over 45 minutes in human beings. The most common causes are persistent spasm of a significantly narrowed coronary artery (> 75 %) or rupture of an atherosclerotic plaque which leads to a vessel thrombosis. The healing of MI is a dynamic biological process initiated by induction of acute inflammatory response followed by formation of granulation tissue and deposition of extracellular matrix leading to a subsequent scar formation. This sequence of events is termed myocardial remodeling. MI is often clinically associated with potentially life threatening complications. An acute infarction may lead to severely impaired cardiac output and further compromise the coronary ischemia with extension of the infarcted area. The difference in conduction velocity between injured and uninjured tissue can trigger re-entry arrhythmias or a feedback loop that is believed to be the cause of many lethal ventricular tachycardia or fibrillation events. In addition, adverse myocardial remodeling may result in the formation of a ventricular aneurysm that can rupture with catastrophic consequences.

Remodeling after MI is generally associated with left ventricular dilation and dysfunction leading to development of a terminal heart failure with a high mortality (Pffefer et al., 1979). An early reperfusion is however, associated with a rapid formation of stable scar and better prognosis. Therefore, most experimental and clinical therapies have mainly focused on early reperfusion and limiting the infarct size (Amber et al., 2006; Lunde et al., 2006).

Conservative treatment for coronary artery disease usually involves lifestyle changes and medication. In cases of highly impaired blood flow an angioplasty with stent placement or a coronary artery bypass surgery are indicated. Despite advances in medical and interventional therapies, the prognosis of millions of patients with acute myocardial infarction (AMI) and ischemic cardiomyopathy has yet to improve significantly.

1.2 Myocardial remodeling after infarction

The irreversibly damaged myocardium undergoes a series of structural and functional changes that ultimately lead to formation of a fibrous scar, myocardial remodeling. Myocardial remodeling is closely related to "infarct expansion" which may continue after the necrosis has reached its ultimate size and where the left ventricle dilates probably due to increased wall stress (Aikawa et al., 2000). Subsequently, this is followed by progressive remodeling in the non-infarcted (remote) myocardium (Sam et al., 2000). These early changes are reversible to a certain extent and the myocardium remains relatively plastic until late remodeling leads to a formation of a stable scar tissue. The extent of morphological and functional changes is depending on a number of factors, e.g. therapy applied for revascularisation, time point of reperfusion, the size of area at risk, etc. Since most of the recent advances in our understanding of myocardial remodeling are based on animal models, the further explanation of underlying pathomechamisms is based on animal experimental data.

1.3 Mouse model of reperfused myocardial infarction

Experimental models of MI have been developed in pigs, dogs, rats and mice. Large animal models have been extensively used to study the mechanisms involved in myocardial injury and repair (Jugdutt et al., 1976; Michael et al., 1979) and have significantly contributed to our basic understanding of the myocardial infarction pathology. However, large animal studies have

limitations in investigating the functional role of specific genes and pathways involved. Therefore, recent advances in transgenic and gene targeting approaches allowed sophisticated genetic manipulations in order to investigate injury and repair following MI (Chien et al., 1996). For reasons of technical and economic consideration, these experiments are largely confined to the mouse (James et al., 1998; Franz et al 1997). To capitalize on these advances in gene targeting technology murine models of experimental MI have been developed in order to examine different aspects of regulation of inflammatory mediators during reperfusion, metabolic changes in cardiomyocytes, angiogenesis, collagen deposition during scar formation etc. Most of the studies involving mice and rats utilize models of coronary occlusion without reperfusion. Since current clinical practice is aiming to reach an early reperfusion of an occluded disease, these models may not be the best option for translational research. Nossuli et al described for the first time the use of a closed-chest mouse model of myocardial ischemia and reperfusion that allows a temporary total occlusion and subsequent reperfusion of the LAD at any time after instrumentation (Nossuli et al., 2000). This method allows dissipation of the acute trauma and inflammation of the initial surgery, which may significantly influence experimental results when investigating inflammatory response during myocardial ischemia and reperfusion (MI/R). The acute surgical trauma may not only increase cytokine background, but also may accentuate or prime the inflammatory response and thus cause significantly greater data variability. A period of 7 to 10 days between the initial surgery and the MI/R has proved to be sufficient to avoid these effects.

Using this model as a basis Dewald et al described a model of reperfused myocardial infarction in mice (Dewald et al., 2004). The reperfused infarction was associated with rapid infiltration of the injured myocardium with inflammatory cells and accompanied by phagocytosis of necrotic cardiomyocytes after 24 hours of reperfusion. After 72 hours of reperfusion, infarcted area showed a complete replacement of injured cardiomyocytes with granulation tissue. In the process of tissue fibrosis and remodeling fibroblasts differentiate into myofibroblasts while expressing contractile elements such as α-SMAc (Frangogiannis et al., 2002). Activated myofibroblasts are dynamic regulators of the fibrosis through the synthesis of extracellular matrix proteins and metalloproteinases. The myofibroblasts occur also in a transient fashion since after 7 to 14 days of reperfusion the mature mouse infarction shows only a low myofibroblast content.

The remodeling may also involve changes in ECM in the remote myocardium (Weber et al., 1994). Alterations in ECM, in particular increased collagen accumulation (Lutgens et al.,1999;

Van Kerkhoven et al., 2002) and changes in the activity of matrix metalloproteinases and tissue inhibitors of metalloproteinases have been observed in the remote myocardium after infarction (Petersons et al., 2000). These ECM changes may contribute to LV chamber dilation via myocyte lengthening and/or slippage (Olivetti et al., 1990; Gerdes et al., 1995; Weber et al., 1994). Even though remodeling of ECM is mainly performed by myofibroblasts and dependent on their ability to proliferate and produce ECM components it is substantially dependent on the preceding inflammatory response in infracted myocardium (Darby et al., 1990). Several of inflammatory mediators and cells, e.g. macrophages regulate not only the inflammatory response, but also the transition into remodeling and scar formation.

1.4 Inflammatory reaction after myocardial infarction

MI and reperfusion are associated with a strong transient inflammatory response preceding remodeling into stable scar formation. Myocardial necrosis induces complement activation and free radical generation and triggers a cytokine cascade with subsequent upregulation of other inflammatory mediators, e.g. chemokines. Interleukin-8 and C5a are released in the ischemic myocardium, and seem to play an important role in mediating neutrophil and monocyte recruitment in injured myocardium (Mehta et al., 1999; Frangogiannis et al., 1996). The main function of neutrophils appears to be removal and degradation of dead cardiomyocytes and tissue debris. Granulocyte infiltration is followed by chemotactic attraction of monocytes and lymphocytes cells , which provide a rich source of cytokines and growth factors necessary to support fibroblast proliferation and neovessel formation. Several animal studies offer more details on the role of reperfusion in ventricular remodeling. For example, late reperfusion in dog infarction resulted in accelerated inflammatory response and increased rate of effective infarct repair (Richard et al., 1995). Similar studies done in rat suggested that late reperfusion was associated with limited infarct expansion (Boyle and Weisman, 1993).

1.5 Mediators of inflammatory response

The inflammatory response after MI/R involves a number of pro and anti-inflammatory mediators. Most prominent factors are pro-inflammatory cytokines, e.g. TNF-α, and interleukin 1-β, whereas interleukin 10 acts predominantly in anti-inflammatory fashion. Even though transforming growth factor beta isoforms belong to the cytokine family, they exhibit their action during the resolution of inflammatory response and subsequent myocardial remodeling. In the last few years a novel subfamily of cytokine termed chemokines has been described and there is a growing evidence of their role in the fine-tuning of both the inflammatory response and the remodeling process. The expression of cytokines, chemokines and adhesion molecules is transient in reperfused mouse infarction, since it decreases significantly after 24 hours of reperfusion probably due to rapid up-regulation of anti-inflammatory IL-10 and TGF-ß (Dewald et al., 2004). Recent investigations using experimental model of MI demonstrated marked induction of CC-chemokine ligand 2 (CCL 2 or MCP 1), CCL 3 and CCL 4 (MIP 1α and 1β, respectively) in infarcted hearts supporting a role for these chemokines in leukocytes recruitment, angiogenesis and healing (Frangogiannis et al., 2004; Frangogiannis et al., 2001).

Tumor necrosis factor α

TNF-α is expressed at low concentrations in an uninjured heart and it is mainly located to the vascular endothelium. TNF-α is released from macrophages, monocyte and mast cells within minutes after myocardial ischemia (Frangogiannis et al., 1998; Bellisari et al., 2001), representing an upstream cytokine responsible for initiating the inflammatory cascade. Its concentration increases within the area at risk (Frangogiannis et al., 1998; Gurevitch et al., 1996; Irwin et al., 1999) with prolongation of ischemia and development of cardiomyocytes necrosis. Also the TNF-α-concentration increases in the surrounding viable portions of the myocardium (Dörge et al., 2003; Ono et al., 1998; Thielmann et al., 2002) probably due to an increased stretch of cardiomyocytes (Kapadia et al., 1997). Experimental findings suggested that TNF-α may induce a cytoprotective signal capable of preventing or delaying the development of myocyte apoptosis following MI (Kurrelmeyer et al., 2000).

Interleukin 1β

IL-1β plays a central role in regulating inflammatory and fibrotic responses: by inducing synthesis of other proinflammatory mediators, by promoting leukocyte infiltration and activation, and by modulating fibroblast function. Administration of an anti-IL-1β neutralizing antibody in the acute phase of non-reperfused murine MI was detrimental, resulting in reduced collagen accumulation in the scar and attenuated adverse remodeling (Hwang et al., 2001). In contrast inhibition of IL-1-mediated effects through over expression of IL-1-receptor antagonist decreased cardiomyocytes apoptosis, reduced inflammation and decreased myocardial injury after reperfused infarction (Suzuki et al .,2001).

Interleukin 10

IL-10 is a prominent cytokine synthesis inhibitory factor and primarily a product of Th2 cells and endotoxine–stimulated monocytes (Mossmann et al., 1994). IL-10 inhibits the production of IL-1α, IL-1β, TNF-α IL-6, and IL-8 by LPS activated monocytes, thus suppressing the inflammatory response. IL-10 may have a significant role in extracellular matrix formation by modulating expression of metalloproteinase's and their inhibitors (Lacraz et al., 1995). Additional investigations indicated that IL-10 deficient mice show enhanced neutrophils recruitment, elevated plasma levels of TNF-α and high tissue expression of ICAM-1 (Yang et al .,2000). Thus IL-10 may have a protective role after MI/R through the suppression of the acute inflammatory process.

CC-chemokine ligand 2

CCL 2 is the major chemokine involved in recruitment, activation and function of monocytes and macrophages. It also participates in the regulation of T cells and NK cells, and it has been implicated in diseases characterized by monocyte-rich infiltrates. CCL 2 has been shown to be up regulated in experimental MI models and promotes mononuclear cell recruitment into the infarcted heart (Dewald et al., 2004). Anti–CCL 2 gene therapy has improved survival and attenuated LV dilatation and dysfunction in a murine MI model (Hayashidani et al., 2003). Furthermore, the targeted deletion of its receptor CCR 2 in mice also improved LV dilatation and dysfunction after MI, suggesting a deleterious role for CCL 2 in post infarct LV dysfunction

and remodeling (Kaikita et al., 2004). The angiogenic and cardioprotective effects of CCL 2 have also been reported. (Salcedo et al., 2000; Tarzami et al., 2002).

Dewald et al, recently demonstrated that CCL 2 gene disruption led to decreased and delayed macrophage infiltration in the healing infarct and delayed replacement of injured cardiomyocytes with granulation tissue (Dewald et al., 2005). They also showed that CCL 2 deficiency had decreased the expression of several cytokines, e.g. TNF-α, IL-1α, IL-1β, IL-10, and transforming growth factor (TGF)-β, and diminished myofibroblasts accumulation. Thus suggested a crucial role of CCL 2 in myocardial healing after MI. Martire et al, recently reported that cardiac over expression of CCL 2 could prevent myocardial damage against shorter I/R injury (Martire et al., 2003).

CC-chemokine ligand 4

CCL 4 is induced in ischemic tissues and exhibits its chemoattractant properties mainly on mononuclear cells. A robust induction of CCL 4 was noted in experimental models of myocardial (Dewald et al., 2004) and cerebral (Kim et al., 1995) ischemia and reperfusion, and it may critically regulate inflammatory cell recruitment. (Frangogiannis et al., 2004). CCL 4 receptors, e.g. CCR 1, CCR 5, are also significantly induced after myocardial infarction (Dewald et al., 2005).

Nossuli et al reported that after one brief episode of myocardial I/R, oxygen radicals lead to a strong up-regulation of CCL 3 and CCL 4 mRNA in a TNF-α independent manner in the venular endothelium of the reperfused myocardium (Nossuli et al., 2000). Another report has implicated human CCL 4 in the induction of the adhesive properties of T-lymphocytes and found this molecule to be localized to lymph node endothelium (Tanaka et al., 1993). They also showed that CCL 4 is most effective at augmenting adhesion of CD 8^+ T cells to the vascular cell adhesion molecule (VCAM-1), and that it is also bound to the endothelium. By now, the exact function and the interactions of these chemokines are not well understood in the pathogenesis of ischemic injury and tissue repair.

1.6 Mediators of Myocardial Remodeling and Scar Formation

ECM is controlled by a system of proteolytic enzymes, the matrix metalloproteinases (MMP) and their inhibitors, the tissue inhibitors of MMPs (TIMP). An MMP expression is up-regulated in infarcted myocardium (Cleutjens et al., 1995; Lu et al., 2000) and has a prominent role in ECM remodeling. During the early stages of remodeling activated MMPs degrade the pre-existing ECM by disruption of the fibrillar collagen network. Subsequently the inflammatory cells migrate into the infarct tissue to remove the necrotic cardiomyocytes and in release again the MMPs, cytokines, growth factors and angiogenic factors. Studies showed that administration of MMP inhibitors and targeted deletion of MMP9 attenuated left ventricular enlargement in MI (Rohde et al., 1999; Ducharme et al., 2000).

The myocardial remodeling involves myofibroblasts and is dependent on their ability to proliferate and produce ECM components. Myofibroblasts are regarded as major contributors to scar formation both indirectly by regulating scar formation via secretion of fibrogenic growth factors (Campell et al., 1997; Katwa et al., 2003), and directly by collagen secretion (Cleutjens et al., 1995). Again, the formation of a stable scar is dependent on interaction between macrophages and myofibroblasts, which is not completely understood yet. Among the most prominent mediators in this process are transforming factor β isoforms and osteopontin.

Transforming Growth Factor β (TGF-β)

TGF-β is produced by various cells including B and T cells, macrophages, tumor cells and myocardial cells. Studies investigating the repair of rat cutaneous wounds demonstrated that TGF-β isoforms 1 and 2 (Shah et al., 1994) promote excessive deposition of ECM proteins that lead to scar tissue formation. In contrast, exogenous application of TGF-β3 to these wounds reduced ECM protein deposition and scarring (Shah et al., 1995). TGF-ß isoforms 1, 2 and 3 exhibited differential expression in mouse infarcts: TGF-β1 and β2 were induced after 3 hours and their expression significantly decreased after 3 to 7 days of reperfusion, whereas TGF- β3 showed a delayed and sustained induction after 3 to 7 days (Dewald et al., 2004). Differential expression of TGF-β isoforms in infarcts may regulate ECM remodeling in view of its ability to enhance collagen synthesis, angiogenesis and compensatory myocardial hypertrophy. Increased and sustained TGF-β3 synthesis during maturation of the scar may prevent excessive accumulation of collagen in the injured heart. TGF-β1 expression appears to be important in

regulating the phenotypic changes associated with myofibroblast differentiation (Desmouliere et al., 1993). Furthermore, TGF-β diminished the amount of superoxide anion in the coronary circulation, maintained and/or restored endothelial-dependent coronary relaxation and limited the size of cardiac damage (Lefer et al., 1990). This protective action of TGF-β can be attributed to its anti-inflammatory and anti-TNF-α actions.

Osteopontin (OPN)

OPN is an ECM protein, although it was first isolated from mineralized bone matrix; it has since been shown to be synthesized by several cell types, including cardiac myocyte, micro vascular endothelial cells, and fibroblasts (Giachelli et.al., 1995; Ashizawa et al, 1996). OPN appears capable of mediating diverse biological functions including cell adhesion, chemotaxis, and signalling (Giachelli et al., 1995; Denhardt et al., 1993). OPN has also been shown to interact with fibronectin and collagen suggesting its possible role in matrix organization and/or stability (Kaartinen et al., 1999; Mukherjee et al., 1995). OPN has been reported to play a critical role in the generation of interstitial fibrosis in the kidney after obstructive nephropathy (Ophascharoensuk et al., 1999). OPN is one of the factors responsible for the recruitment of a macrophage-rich leukocyte infiltrate into the interstitium of the post ischemic heart. Also, due to a strong expression on terminally differentiated macrophages in postischemic myocardium, it is considered as a marker of mature macrophages (Murry et al., 1994). Persy et al. demonstrated macrophage infiltration and tubule interstitial fibrosis were significantly reduced in the absence of OPN protein in an experimental renal study (Persy et al., 1999).

1.7 Cellular therapy of ischemic heart

The critical loss of functional cardiomyocytes causes a severe deterioration of ventricular function resulting in heart failure. Because terminally differentiated cardiomyocytes lack prominent regenerative capacity heart transplantation remains the best therapeutic option for terminal heart failure. Still, the increased demand for transplantation is confronted with a shortage in donor organs, thus leading to a strong demand on alternative therapies. A new therapeutic approach is CCM in which appropriate donor cells are delivered to the injured

myocardium. This approach targets the pathophysiological basis of congestive heart failure by attempting to regenerate the damaged myocardium through transplantation of healthy cells. Many cell types have been transplanted into injured myocardium: embryonic cardiomyocytes (Roell et al., 2002), fetal cardiomyocytes (Sakakibara et al., 2002), skeletal muscle calls (Reinecke et al., 2002), mesenchymal stem cells (Beyer et al., 2006; Wang et al., 2007), etc. Up to this moment there is an ongoing controversial debate over which cell type may be the best suitable for CCM (Laflamme et al., 2005; Murry et al., 2005).

In the past few years, attention has be drawn to transdifferentiation of bone marrow cells into cardiomyocytes (Orlic et al., 2001) as a source of cardiomyocyte replacement in damaged heart, either through generation of cardiomyocytes or through angiogenesis with improved cardiac function. These initial findings have provoked extensive follow-up studies.

Studies on BMSC therapy in experimental animal models (Kudo et al., 2003) and patients with AMI (Strauer et al., 2002; Chen et al., 2004) have shown an improvement in cardiac function and thereby promoted the safety and feasibility of this approach. Other studies demonstrate that BM derived hematopoietic cells do not transdifferentiate into cardiomyoplasty in infarcted myocardium (Nygren et al., 2004; Murry et al., 2004). Other groups suggested that paracrine effects originating from the transplanted cells could be responsible for the cardioprotective effects (Balsam et al., 2004). In addition to the above mentioned experimental evidence, the BMSCs may contribute to the repair the ischemic myocardium also by angioblast-mediated vasculogenesis (Kocher et al., 2001; Kawamoto et al., 2001), by prevention of apoptosis of native cardiomyocytes, or by direct regeneration of the lost cardiomyocytes (Orlic et al., 2001). The underlying mechanisms of myocardial improvement are not well understood despite of fast growing number of experimental and clinical studies.

Different routes of cell administration have been used in human and animal studies:

1. ***Intramyocardial injection***: Donor cells are directly injected during open-heart surgery and minimally invasive thoracoscopic procedures. Here the cell availability is not limited by uptake from the circulation or by embolic risk. The remaining risk of ventricular perforation limits the use of direct needle injection into freshly infarcted hearts.
2. ***Intracoronary injection***: Donor cells are delivered diffusely by a single injection of cells via coronary artery, either through coronary catheterization or injected into aortic root

during cardiac surgery under the cardiopulmonary bypass. Different cell type were administered in clinical studies, e.g.BMMNC, EPC and MSC (Abbott et al., 2004; Assmus et al., 2002; Wollert et al., 2004). The results indicated that intracoronary transfer of BM cells was not only safe, but also enhanced regional wall motion (Schachinger et al., 2004; Wollert et al., 2004)

3. ***Systemic intravenous injection***: This least invasive, simple technique brings the cells into the blood steam and they reach the myocardium via the coronary circulation (Chen et al., 2001; Chen et al., 2003). The cells are able to home in and localize within and around the infarcted segment of myocardium. The major pit fall is the lack of control over the amount of cells homing to the ischemic heart and possible cleavage of them in the spleen and/or liver.

In the light of growing clinical practice aiming for early reperfusion of MI there is also a growing need for fast availability of large number of cells for cardiomyoplasty. The ongoing clinical and experimental studies show encouraging results, but leave several unsolved problems especially in the area of cellular interactions and mediators involved. In order to better understand the pathomechanisms of myocardial remodeling and thus to improve the postinfarction healing we combined our well-established models of reperfused MI and cellular therapy in the heart for investigation of the following hypothesis.

1.8 Hypothesis

We postulated a role for whole bone marrow cells in promotion of active interstitial remodeling in a mouse model of reperfused MI.

2 Materials and methods

2.1 Animal surgery

Male and female WT C57/BL6 mice (Charles River laboratories), 10 to 16 weeks of age (18 to 22 g body weight) **.** All experiments were performed in accordance with an approved animal protocol : AZ 9.93.2.10.31.07.051.

In an initial surgery, mice were anesthetized by an intraperitoneal injection (i.p) of sodium pentobarbital (10 mg/g). A closed chest model of reperfused MI was utilized as described below (Dewald et al., 2004). Briefly, after thoracotomy the pericardium was dissected and an 8-0 Prolene suture (Ethicon, Sommerville, NJ) with a U-shaped tapered needle was passed under the LAD coronary artery. The needle was cut from the suture, and the two ends of the suture were threaded through a 0.5-mm piece of PE-10 tubing (Becton Dickinson, Sparks, MD), thus forming a loose snare around the LAD. The PE-10 tubing was previously soaked for 24 hours in 100 % ethanol. Each end of the suture was then threaded through the end of a size 3 Kalt suture needle (Fine Science Tools, Foster City, CA), and exteriorized through each side of the chest wall. The chest was closed with 3 interrupted stitches using 6-0 Prolene. The ends of the exteriorized 8-0 suture were tucked under the skin, after that the skin was then closed with 6-0 Prolene suture **.** At the end, metamizol (100 mg/kg; Novalgin) was given for analgesia in a mixture with cefuroxim as antibiotic prophylaxis i.p. (100 mg/kg, Zinacef; Bristol-Myers Squibb, Munich, Germany. The endotracheal tube was withdrawn, and the animal was kept warm with a heat lamp and allowed to breathe 100 % oxygen via nasal cone until full recovery.

Seven to ten days post instrumentation the animals were anesthetized with 1.5 % MAC isoflurane, and the extremities were taped to a lead II ECG board to measure S-T elevations during I/R protocol. The skin above the chest wall was then reopened, and the 8-0 suture, which had been previously exteriorized outside the chest wall and placed under the skin, was cleared of all debris from the chest and carefully taped to heavy metal picks. Occlusion of the LAD was accomplished by gently pulling the heavy metal picks apart until an S-T elevation appeared on the ECG. The ECG was constantly monitored throughout the entire ischemic interval to ensure persistent ischemia. After one hour of coronary occlusion, reperfusion was achieved by pushing the metal picks toward the animal, cutting the suture, then removing it completely. The mice in

the immediate group received injection into the right or left subclavin vein. Again the skin was closed with 6-0 Prolene. The mice in the later injection group were anesthetized in the same fashion as described above and received the I.V. injection in the same fashion as described.

2.2 Mice groups

Upon initial surgery the animals were assigned to different groups:

- immediately after start of reperfusion immediate injection of either WBM or PBS as control for 7 days of reperfusion and 28 days of reperfusion (n=8 for each groups).
- 72 hours after start of reperfusion injection of either WBM or PBS as control for 7 days of reperfusion and 28 days of reperfusion (n=8 for each groups).

The influence of WBM injection on morphological changes was characterized at time points 7 and 28 days of reperfusion, the ventricular function after 28 days reperfusion, and the differences in expression of molecular markers were investigated after 7 days of reperfusion (n=8 for each groups). Hearts were harvested after reperfusion period using overdose of pentobarbital. The animals in histological groups underwent measurement with LV-catheter prior to heart excision as described below.

2.3 Whole bone marrow cell isolation and preparation

The bone marrow cells were obtained from both left and right lower limbs (tibias and femurs) of commercially available GFP- ubiqutine mice (C57/ BL6 background, Jackson Labs). Briefly, the bone was cleaned with paper towel soaked with 75% ethanol to remove the adhesion muscle and tissue and then further processed under the cell culture hood. Tibia and femur were separated and the bone marrow was flushed with PBS using a 27- gauge needle and then filtered through 70 µm nylon mesh cell strain. The cells were then centrifuged (5 minutes at 2000 rpm) and the cell count was performed in Thoma chamber (Paul Marienfeld GmbH & Co. KG, Lauda-Koenigshofen Germany). The cells from the two quadrant field under microscope were counted, the mean was

calculated and the cells were diluted to a concentration of $5x10^6$ / 100 µl in PBS. 100 µl of cell suspension or PBS alone were injected intravenously as described above.

2.4 Left Ventricular catheter measurement

The hemodynamic measurements were performed using Aria-system (Föhr Medical instruments, Seeheim-Ober-Beerbach) after 28 days reperfusion in anaesthesisized mice as described above. After the right or left carotid artery preparation a 1.4 Fr micro-tipped manometer was inserted into it and advanced into the LV lumen to measure LV dP/dt. Parameters as aortic blood pressure and HR, LV pressure and volume were measured.

2.5 Tissue processing for histology

2.5.1 Tissue embedding in paraffin

The harvested hearts were briefly flushed with cardioplegic solution containing 4 g NaCl, 3.73 g KCl, 1 g $NaHCO_3$, 2 g glucose (all from Berlin Chemie, Berlin, Germany), 3 g 2,3-butandion monoxime (Sigma-Aldrich, Munich, Germany), 3.8 g ethylenglycol tetra acetic acid (Sigma), 0.2 mg nifedipine (Sigma), and 10 ml heparin (1000 IU/ml; Ratiopharm, Ulm, Germany), all of which were dissolved in 1 L of isotonic NaCl (Berlin Chemie). Blood remnants were washed out of the ventricles and then fixed in zinc-buffered formalin for 18 to 24 hours (Z-fix, 4%; Anatech, Battle Creek, MI, USA)**,** then the hearts were embedded in cassettes and rinsed under the running cold water for 2 to 3 hours, after that they were put in an automatic embedding machine (STP-120, Microm international Gmbh, Walldorf). The hearts underwent dehydration procedure by using high concentrations of ethanol and finally xylene. After infiltration with paraffin (2 hours at 60 °C) the hearts were embedded into paraffin by specific orientation in the holding cassette (Microm-1 EC350). The paraffin blocks were cut with microtome (SM 2000 R, Leica Microsystems Gmbh). The hearts where cut from basis to apex, at every 250 μm, a set of ten 5 μm sections were mounted on glass slides (Silane treated surface, HistoBond®, Marienfeld, Lauda-Königshofen, Germany). A drying period in a dehumidifying chamber at 42 °C followed

overnight. The first section was stained with haematoxylin and eosin for initial evaluation. Myocardial sections below insertion of the papillary muscles were further used for histology and immunohistochemistry.

2.6. Basic histology protocols

2.6.1 Haematoxylin . Eosin

Haematoxylin is basophilic and stains cell nuclei blue, while eosin is acidophilic and stains cytoplasm, connective tissue and other extra cellular substances pink or red. Eosin is strongly absorbed by red blood cells coloring them bright red.

The slides were placed in a slide holder and deparaffinized and rehydrated in:

- Xylen 3 x 10 minutes
- Isopropanol 100% 2 x 5 minutes
- Isopropanol 90% 1 x 5 minutes
- Isopropanol 70% 1 x 5 minutes
- Distilled water 1 x 5 minutes

Haematoxylin staining:

- Haematoxylin 5 minutes
- Tap warm water 5 minutes

Then Eosin staining and dehydration through:

- Eosin 1-2 minutes
- Distilled water Shortly
- Isopropanol 70% Shortly
- Isopropanol 90% Shortly
- Isopropanol 100% 5 minutes
- Isopropanol 100% 5 minutes

- Xylene 3 x 5 minutes

The slides were mounted with cover slip using permount (Merck, Darmstadt, Germany).

2.6.2 Collagen Staining with Picrosirius Red

Picrosirius red stains collagen red on a pale yellow background. Its solution was prepared using 0.1 g of Direct red 80 (Sigma-Aldrich) in 100 ml picric acid solution, left for 5 to 10 minutes and finally filtrated.

Deparaffinization and rehydration as described in 2.6.1.

Sirius red staining:

- Sirius red solution 10 minutes

Dehydration of the sections

- Distilled water 15 dips
- Isopropanol 90% 15 dips
- Isopropanol 100% 15 dips
- Xylen 3 x 5 minutes

The slides were mounted with cover slip using permount (Merck, Darmstadt, Germany).

2.7 Immunohistochemistry

2.7.1 Immunohistochemical staining of macrophages and myofibroblasts

The slides were deparaffinized and rehydrated as described in 2.6.1. The tissue was circled with PAP pen (wax, Labomedic, Bonn, Germany) and rinsed in PBS for 2 minutes.

Sections were stained immunohistochemicaly with the following antibodies: Monoclonal anti-α-SMAC antibody (Sigma, St. Louis, MS, USA) and macrophage monoclonal F4/80 antibody (Serotec, Kidlington, United Kingdom).

Staining was performed using a peroxidase-based technique with Vectastain kit (Vector Laboratories Burlingame, USA,) and developed with diaminobenzidine-nickel (DAB, Vector). The MOM kit (Vector) was used for α-SMAC immunohistochemistry. Slides were counterstained with eosin and examined in a Zeiss microscope equipped with digital camera (AxioCam MRC5, Carl Zeiss, Jena, Germany).

2.7.1.1 Myofibroblast staining protocol

The sections were incubated for 10 minutes in 3 % hydrogen peroxide (blocking the endogenous peroxidase), then incubated for 60 minutes with mouse IgG block (M.O.M Kit) for blocking the non specific binding. The slides were rinsed in PBS (PH 7.1) two times for 5 minutes.

M.O.M protein solution was added to the sections because it has a significant role in reducing the undesired background staining when using a mouse derived antibody in a mouse. After 5 minutes the M.O.M protein was tapped off and then incubated with mouse α-SMAC antibody (Sigma) in the dilution of 1:250 for 30 minutes at room temperature or over night at 4 °C in refrigerator. The slides were rinsed in PBS and incubated with biotin IgG (secondary antibody) for 10 minutes. The slides were rinsed with PBS and incubated with ABC- peroxidase for 5 minutes. In the next step, the slides were incubated with DAB for 5-10 minutes under direct visual control under the microscope and this was stopped by a short rinse in PBS. Finally the slides were counterstained with eosin:

Eosin staining

- Eosin 5 x
- Distilled water 5 x
- Isopropanole 70% 15 x
- Isopropanole 90% 15 x
- Isopropanole 100% 15 x
- Xylene 3 x 5 minutes

The slides were mounted as previously described.

2.7.1.2 Macrophage staining protocol

Macrophages were stained using a similar protocol as for α-smac staining. Incubation in 3 % hydrogen peroxide for 15 minutes was followed by incubation with rat IgG Block (Vectastain) for 30 minutes. IgG–Block was tipped off and incubated with F4/80 antibody at a dilution of 1:250 for 2 hours or over night at 4 °C in refrigerator. The slides were rinsed in PBS 2 x for 5 minutes and then incubated with biotin IgG (1:250 dilution) for 30 minutes. ABC peroxidase incubation followed for 30 minutes, and finally the DAB incubation for 2-10 minutes under visual control. The slides were counterstained with eosin and mounted as mentioned above.

2.8 Immunofluorescent histochemistry of WBM cells

The evaluation of injected WBM cells was performed using immunofluorescent staining techniques for a characterization of GFP-positive cells. The initial procedure for deparaffinisation and rehydration of slides is already described above and the tissue circled with PAP pen. Then the slides were washed 3 times for 10 minutes in PBS. After 10 minutes permeabilisation with 0.5 M aminochloride and 0.25 Triton-X in PBS, the slides were incubated with 5 % BSA or serum (from the same species of secondary antibody) in PBS for 60 minutes to block the unspecific binding. At the next step the slides were incubated with first antibody diluted in 5 % serum over night at 4 ºC (refrigerator) or for 120 minutes at room temperature. After that the sections were incubated with secondary, fluorescent-coupled antibody for 60 minutes at room temperature. The cell nuclei were then stained blue with Hoechst colour solution 33324 (1:1000) and incubated for 20 minutes at 37 ºC. The slides were mounted with cover slip (22 x 50 mm) and DABCO (water based polyvinyl alcohol mounting medium; Sigma) and stored in a dark place.

Primary antibodies:

Target	**Isotype**	**Dilution**	**Company**
GFP	Rabbit IgG	1:50	Santa Cruz
Cardiac troponin T	Mouse IgG	1:200	Neomarkers
α –Smooth muscle actin	Mouse IgG	1:800	Sigma Aldrich
α- Actinin	Mouse IgG	1:400	Sigma Aldrich
CD 45	Rat IgG	1:400	Neomarkers

Secondary antibodies:

Specifically	**FL**	**Isotype**	**Dilution**	**Company**
Mouse IgG	Cy3	donkey	1:400	Jackson Immuno Research
Mouse IgG	Cy5	donkey	1:400	Jackson Immuno Research
Rabbit IgG	Cy2	donkey	1:400	Jackson Immuno Research
Rat IgG	Cy5	donkey	1:400	Jackson Immuno Research

2.9 Evaluation of histological specimen

2.9.1 Quantitative analysis of cellular density

The quantitative analysis was performed in infarcted area, both border zones (anterior and posterior) and non-ischemic myocardium of the septum. Stained sections were photographed with an AxioCam digital camera mounted on a Zeiss microscope; depending on the size of infarction multiple digital images we have taken for each sample. The staining was analysed using analysis software (Soft Image Analysis, Münster).

The macrophage quantification was done by manual count of the F4/80 positive cells at 400X magnification and macrophage density was expressed as cells / mm². Blood vessel density was assessed by counting the number of α-SMAC-positive blood vessel profiles in infarcted and noninfarcted myocardium. The blood vessels were classified as large or small according to their diameter being more or less than 20 μm, respectively. The quantification of GFP-positive cells was performed by manual count of green cells (without staining) under the fluorescent microscope in the normal myocardium, border zones and in infarcted area.

2.9.2 Planimetric evaluation of scar size

Since serial sections were made at 250 mm intervals from the base to apex a planimetric evaluation of the total infarction extension was performed using picrosirius red stained sections. The slides were scanned at 16X magnification using a microscope with a digital camera (Zeiss, Göttingen, Germany) and planimetric evaluation was done with Analysis software. The dense red-coloured area of collagen enabled a precise definition of the scar size and thereby infarct extension. Using same slides the endocardial and epicardial surface area were measured as well. The infarct size (%) was calculated as infarcted endocardial surface area divided by the total endocardial surface area and multiplied by 100.

$$\textit{Infarct size \%} = \frac{\textit{Infarcted endocardial surface area}}{\textit{Total endocardial surface area}} \textit{X 100}$$

2.10 Microscope hardware

1- Stereo microscope Leica MZ 16F (Leica Microsystems GmbH, Solms, Germany), equipped with a Schott KL 1500 LCD 150 watt halogen cold light source and a HBO103 fluorescent lamp and a FITC-band filter. The images were taken with a Jen Optic ProgRes C10 plus camera (Jen Optic AG, Jena, Germany) on the Jen Optic attached software ProgRes Capture.

2- Fluorescent microscope Zeiss Axiovert 200M with ApoTome (CarlZeiss Micro Imaging, Oberkochen, Germany) and a fluorescent lamp XBO75 and long pass filters for EGFP, Cy3, Cy5 and Hoechst (AHF Analysis Technology AG, Tübingen, Germany). The photographs were taken with a Zeiss AxioCam MRm on the Zeiss Axio Vision software.

3- Fluorescent microscope Zeiss Axiovert 40 CFL with the HBO50 fluorescent lamp and band long pass filter for FITC. The pictures were taken with Canon power shot G5 Digital Camera (Canon Deutschland GmbH, Krefeld, Germany).

4- Light microscope Zeiss Axiovert (Carl Zeiss,Oberkochen, Germany) with Carl Zeiss camera MRc5 (Oberkochen, Germany).

5- Light microscope Olympus BX41 (Olympus, Hamburg, Germany) equipped with digital camera Olympus DP70 (Olympus)

2.11 Molecular biology protocols

2.11.1 RNA extraction

All solutions for RNA analysis were made with DEPC- treated water (Ambion, Darmstadt, Germany). Plastics were decontaminated with 70 % ethanol and RNase AWAY (Molecular BioProducts, San Diego, CA, USA) to remove nucleases and DNA contamination.

Total RNA was isolated from the whole mouse heart. Whole hearts were transferred from the RNAlater-Solution (Qiagen) into a 15 ml Falcon tube with 2 ml Trizol Reagent (Invitrogen). Hearts were homogenized with a TissueTearer (ART-MICCRA D-1, Mülheim, Germany) on highest speed until the whole heart was homogenized. After each homogenization, the TissueTearer was cleaned with 0.1 % SDS–solution once and DEPC-treated water twice; solid pieces were removed with a sharp instrument. For RNA extraction, 0.2 ml chloroform (Sigma) was added to the homogenate. After shaking for 15 seconds, the mixture was incubated on ice for 15 minutes and then spun at 12,000 g for 15 minutes at 4 ºC. Then the supernatant was transferred to another a fresh Falcon tube. 1 ml ice-cold isopropanole (Roth; kept at -80 °C) was added and by inverting 20 times the solution was mixed well and incubated for two hours at -20 °C. Then, the solution was spun at 12,000 g for 15 minutes at 4 °C and the supernatant was decanted. 2 ml ice-cold (-20°C) 75 % ethanol were added. The sample was again spun at 12,000 g for 15 minutes at 4 °C. The supernatant was decanted again and the pellet was air-dried for 10 minutes by putting the tube upside down on a Kimtech precision wipe (Kimberly-Clark). Then the tube was wiped out around the pellet with an autoclaved cotton-tipped applicator (Puritan, Guilford, USA). Air-drying proceeded for about another 10-20 minutes until the pellet was totally dry. The RNA pellet was then resuspended in 0.2 ml DEPC-treated water. After incubation for 10 minutes on ice, the solution was resuspended by pipetting.

2.11.2 RNA purification

We added 200 µl of liquid sample to the same volume of RNA Lysis solution, which was prepared freshly for each use by adding 1 % of 2-mercaptoethanol to the same volume of 100 % ethanol. The solution was vortexed and quick spun, and then transferred to the RNA spin cartridge for another spin at 12.000 g for 15 seconds at room temperature. The flow-through was discarded and the cartridge re-inserted in a new tube. We added buffer 1 to the spin cartridge, and

spun at 12.000 g for 15 seconds at room temperature. The flow–through was discarded again, and the spin cartridge placed into a clean RNA wash tube provided in the kit. Wash buffer II was added to the spin cartridge, and centrifuged at 12.000 g for 15 seconds at room temperature. The flow–through was again discarded the cartridge reinserted in the tube .The spin cartridge was spun at 12.000 g for 3 minutes at room temperature to dry the membrane with attached RNA. The collection tube was discarded and the cartridge placed into a RNA recovery tube. The RNA sample was eluted by adding 106 µl of RNAse-free water to the centre of the spin cartridge, and incubated at room temperature for 1 minute, and then spun for 2 minutes at 12.000 g at room temperature. Quantification and purity of RNA was assessed by A260/A280 UV absorption using Nanodrop Spectrophotometer, and RNA samples with ratios above 1.9 were used for further analysis.

2.11.3 Reverse transcription protocol

We prepared the master mix components as shown in the next table:

Component	Volume (µl)
10 x reverse transcriptase buffer	5
25 x dNTPs	2
10 x random primers	5
Multi Scribe Reverse Transcriptase (50/µl)	2,5
RNase Inhibitor (200U/µl)	2,5
Nuclease free water	8
Total	25

25 µl of the master mix were added to 25 µl of the sample. The solution was mixed well by pipetting up and down, vortexed , quick spun and then placed in the thermocycler.
Thermocycler was programmed using following steps:

	Step 1	Step 2	Step 3	Step 4
Temperature	25 °C	37 °C	85 °C	4 °C
Time	10 min	120 min	5 sec	Endless

2.11.4 Real time PCR

We cleaned the desk and pipette with the RNase AWAY (Molecular BioProducts) and ethanol after every pipetting run. For each gene one tube containing negative control (NTC) and another tube with calibrator (CAL) were inserted.

Every sample was measured in triplets, i.e. three measurements of each sample and gene. The previously prepared aliquots of 25 µl cDNA from – 20 °C were vortexed and quick spun. For every sample and the CAL 3 x 6,65 µl cDNA and for NTC 6,65 µl cDNA was pipetted on ice. One master mix was prepared for each gene:

- 3 x 15 x 5 µl Taqman Universal PCR
- 3 x 15 x 1,5 µl Taqman Gene Expression Assay
- 3 x 15 x 2,5 µl H_2O

Mixed well by vortexing and quick spin.

After that 27 µl of master mix were pipetted to 6,65 µl of the sample and control and mixed well by spin at 2000 rpm. In a 384-well plate 3 x 10 µl of the sample-master- mix solution was pipetted according to a specified scheme. The plate was covered with optical adhesive film (Micro Amp, Applied Biosystems, Foster City, USA) and then spun at 2000 rpm for 2 minutes. The plate was placed into the Real-Time cycler (AB 7900HT, Applied Biosystems) with following programme:

	Step 1	Step 2	Step 3	Step4
Temperature	50 ºC	95 ºC	95 ºC	60 ºC
Time	2 minutes	10 minutes	15 seconds	1 minute

The data readout (Ct-method) was performed by the SDS analysis software V2.2 (Applied Biosystems). All samples were normalized to GAPDH as a housekeeping gene and the respective control sample, and shown as ΔΔCt values.

2.12 Statistical analysis

All data are presented as means and SEM. Comparison between the groups was done using analysis of variance with a Student's–Newman-Keuls corrected post hoc analysis. Differences with $p \leq 0.05$ were considered significant.

|3 Results

3.1 Animal surgery results

We performed the initial surgical procedure for placement of the LAD artery suture loop, in a total of 98 C57/BL6 mice. Seven days later all mice underwent the I/R protocol. Nearly 8 mice in each group. Two mice died after WBM cell injection (one mouse in immediate and one in 3 days injection group). A total of 28 mice were excluded from the study because they showed histological evidence of transmural infarction due to initial surgery or no evidence of any infarction. We divided the mice into 4 groups in 7 days of reperfusion and 4 groups in 28 days of reperfusion and the numbers of mice were 8 mice per group.

3.2 Left ventricular function after myocardial infarction

In order to investigate the functional significance of WBM cells a left ventricular catheterization was performed after 28 days of reperfusion in all control and WBM injection groups. We demonstrate the HR and end/systolic pressure, dp/dT max and cardiac output. All data show significant improvements of hemodynamic function in WBM injection groups.

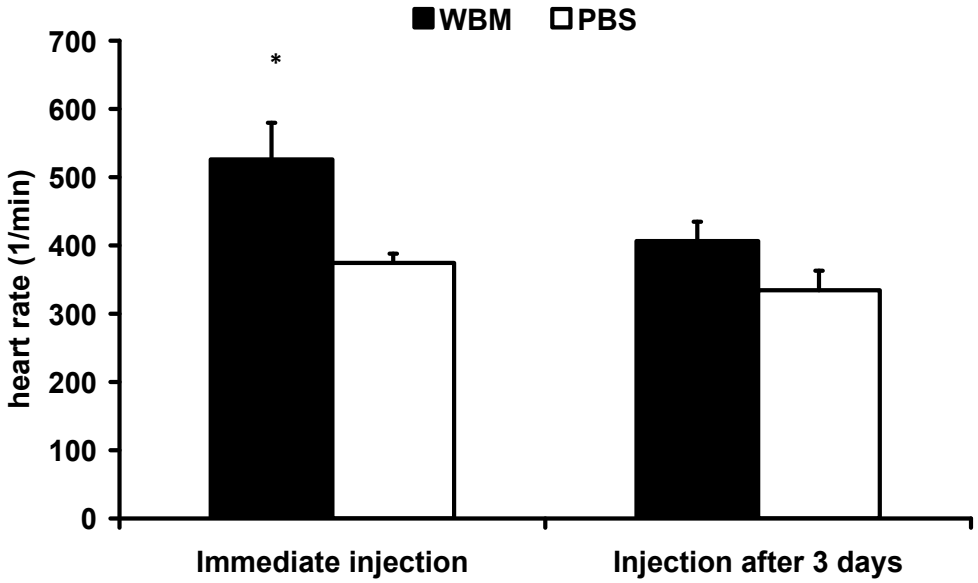

Figure1: *Heart rate in immediate and after 3 days injection of 28 days of reperfusion compared to PBS injection show significant improvements in the heart rate of immediate WBM injections *, p<0.05.*

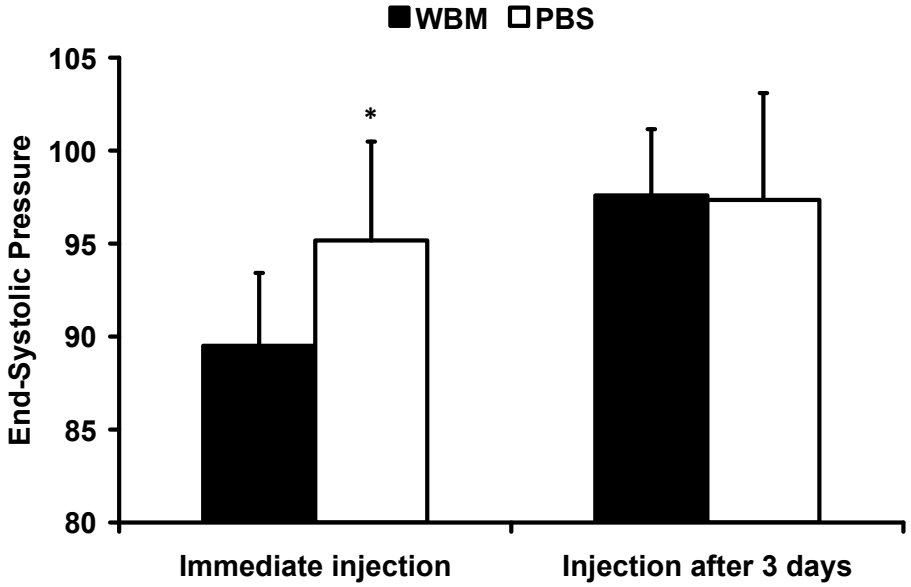

Figure 2*:- End–systolic pressure in immediate and after 3 days of infarction after 28 days of reperfusion compared to PBS injection show significant reduction in the end systolic pressure in WBM immediate injection *, p <0, 05.*

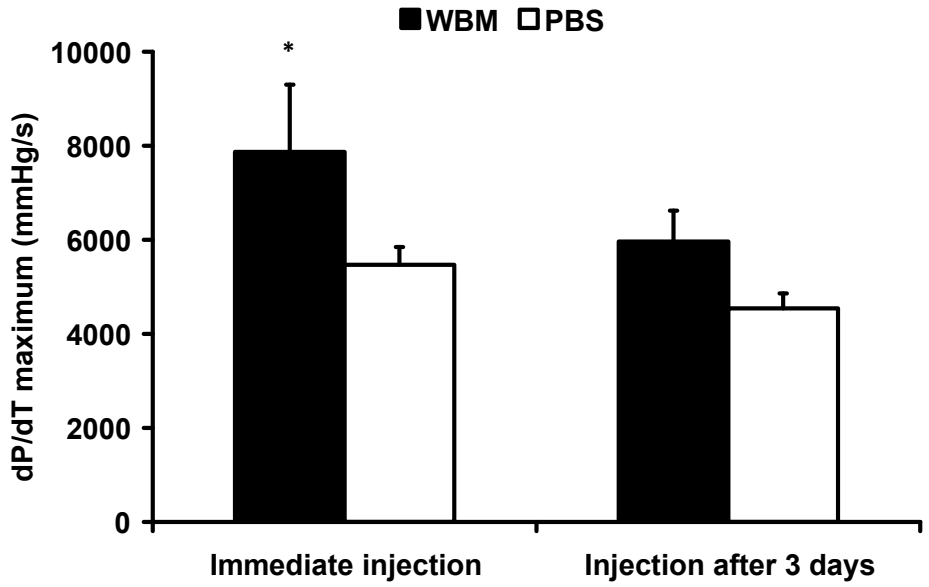

Figure 3:- *dp/dT maximum in immediate and after 3 days injection of WBM cells compared to PBS injection after 28 days of reperfusion, there is a significant increase of the dp/dT maximum in immediate WBM injection *, p <0, 05.*

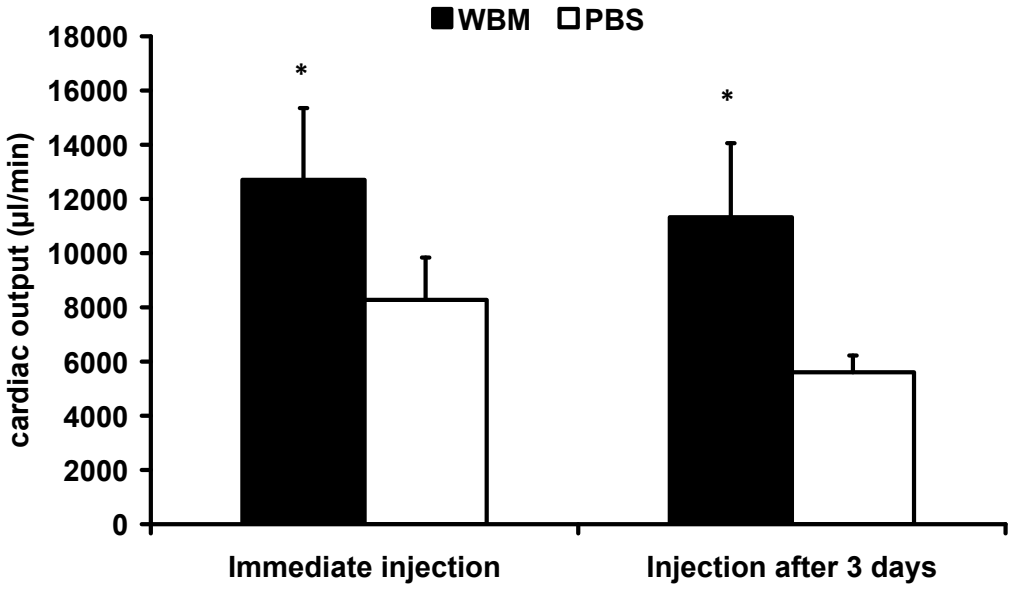

Figure 4*:- Cardiac output measurement in immediate and after 3 days injection of WBM cells after 28 days of reperfusion compared to PBS injection shows a significant improvement of cardiac output in immediate and after 3 days injection of WBM cells *,p <0, 05.*

3.3 Histopathology of myocardial remodeling after cell therapy

3.3.1 Basic histology

Histological evaluation of myocardial infarction using H.E staining revealed after 7 days reperfusion a thin non-transmural scar area with low cellular content and extensive area of replacement fibrosis in PBS injected mice (Figure 5 A, B), which is very comparable with infarction morphology without any injection. The immediate injection of WBM cells led after 7 days of reperfusion to a prolonged granulation tissue formation with high cellularity (Figure 5C). The WBM injection after 3 days of reperfusion was associated with only loose granulation tissue formation and also with persistent high cellular content after 7 days of reperfusion (Figure 5D).

Myocardial scar formation was completed after 28 days of reperfusion in all groups. While the PBS injected hearts showed low cellular content within the compacted non-transmural scar (Figure 6 A, B), the immediately injected WBM cells led to preservation of cardiomyocyte islets in the scar area (Figure 6 C, D). This was associated with persistence of higher cellular content in the scar than in the PBS hearts, while the scar morphology showed compacted fibers and thus appeared comparable between all groups.

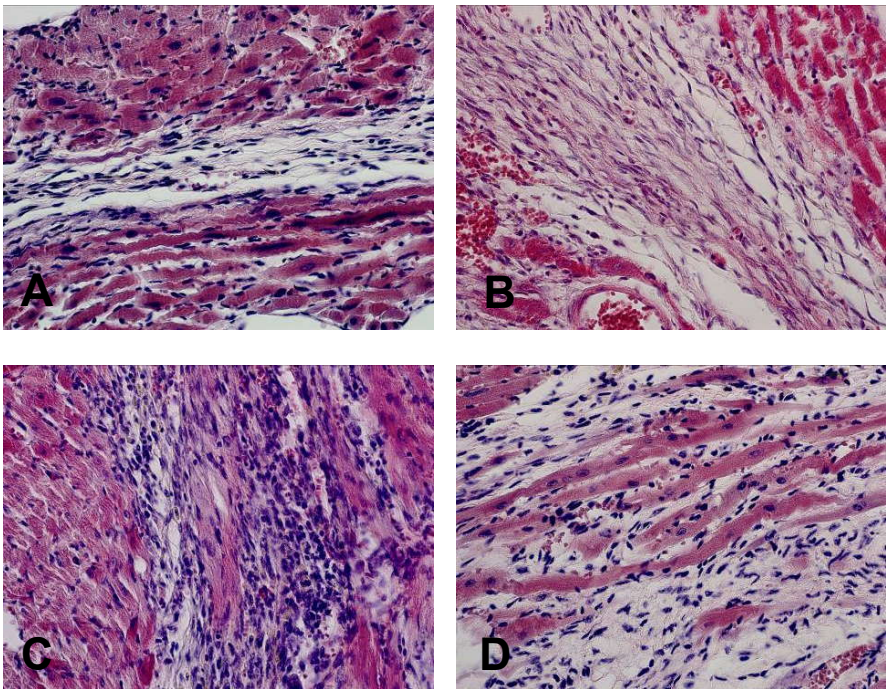

Figure 5: *Basic histology after myocardial infarction I. Hematoxylin-eosin staining shows compacted scar formation after 7 days of reperfusion in control hearts with A) immediate PBS injection and B) PBS injection after 3 days of reperfusion. In contrast, the immediate injection of WBM after MI shows in C) a persistent high cellularity within compacted granulation tissue, while D) WBM injection after 3 days of reperfusion led only to loose granulation tissue formation at this time point.(Magnification, 400X)*

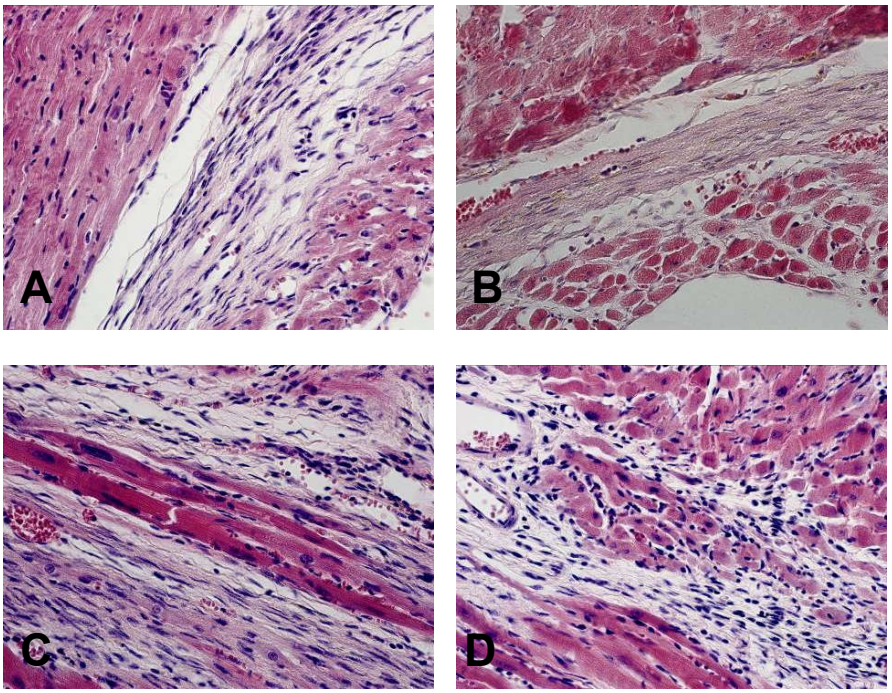

Figure 6: *Basic histology after myocardial infarction II. After 28 days of reperfusion, the representative heart of A) immediate PBS injection and B) PBS injection after 3 days of reperfusion show both a compacted scar tissue. At the same time point C) immediate WBM injection, as well as D) injection after 3 days of reperfusion lead also to a compacted scar, but reveals some scattered cardiomyocyte islets being preserved within it. (Magnification, 400X)*

3.3.2 Collagen deposition in the scar

The collagen staining revealed a rapid scar formation in PBS injected groups (immediate and 3 days injection) after 7 days of reperfusion (Figure 7 A, B). In contrast, the immediate WBM-injection or the WBM cell injection after 3 days of reperfusion (Figure 7 C, D) led to a delayed, but apparently normal collagen deposition, which is loose and not organized at this time point. After 28 days of reperfusion all four groups presented a scar with compacted collagen fibers (Figure 8).

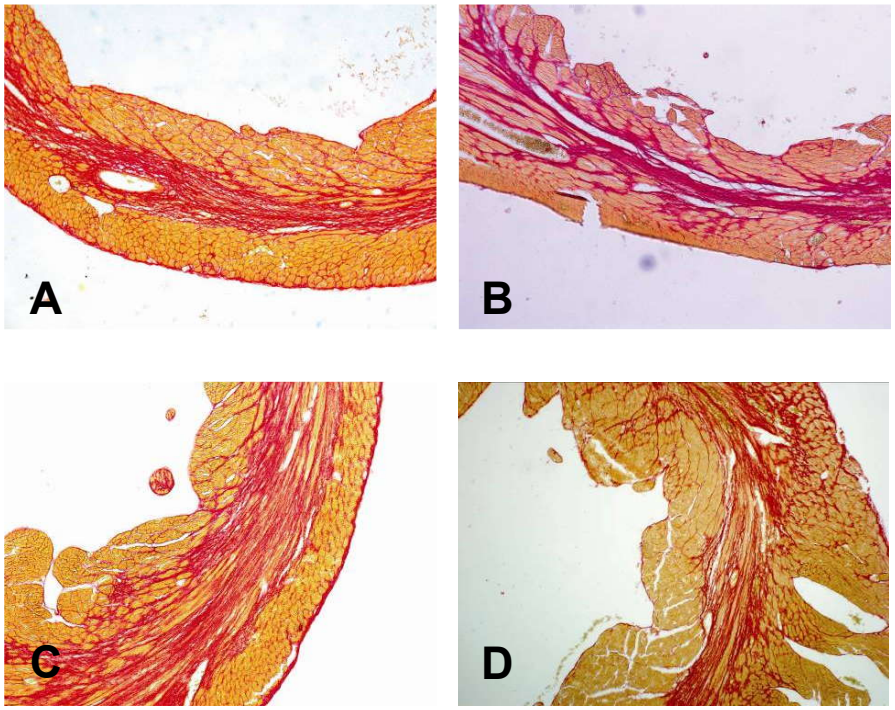

Figure 7: *Collagen deposition in the scar after 7 days of reperfusion. Sirius red staining reveals compacted scar formation, after 7 days of reperfusion in animals with A) immediate PBS injection and B) PBS injection after 3 days of reperfusion. C) Immediate WBM injection and D) WBM injection after 3 days of reperfusion show loose collagen deposition in granulation tissue. (Magnification, 100X)*

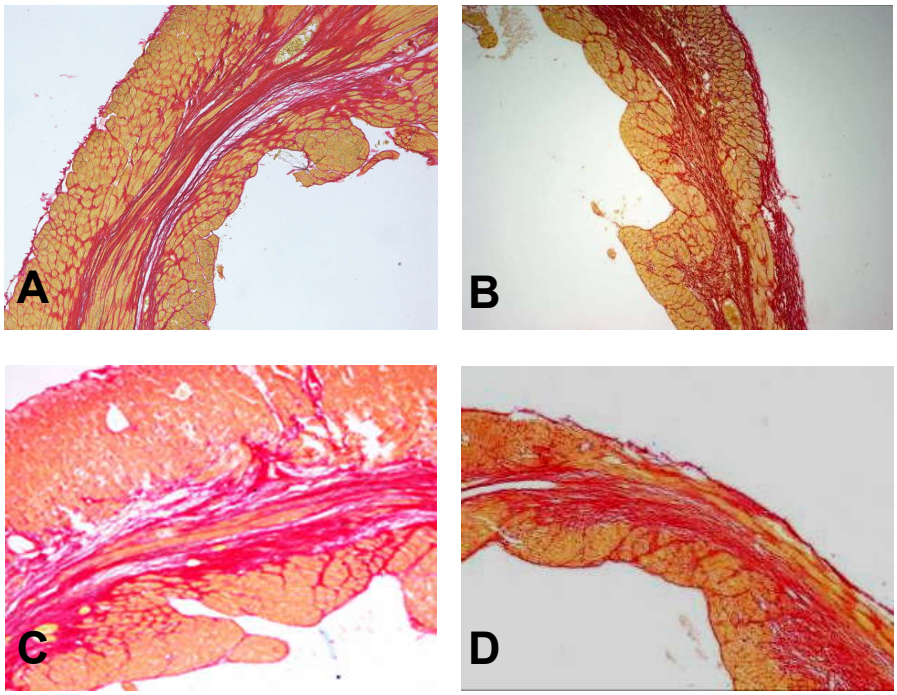

Figure 8*: Collagen deposition in the scar after 28 days of reperfusion. Sirius red staining shows compacted collagen fibers within the scar after 28 days of reperfusion in A) immediate and B) PBS injection after 3 days, as well as C) immediate and D) WBM injection after 3 days of reperfusion. (Magnification, 100X)*

3.4 Scar size

Planimetric evaluation of the scar size based on collagen staining of perfusion fixated hearts revealed a comparable infarction size in both PBS injected groups (Figure 9). WBM cell injected hearts had significantly smaller infarcts than the PBS controls independently of the injection time point.

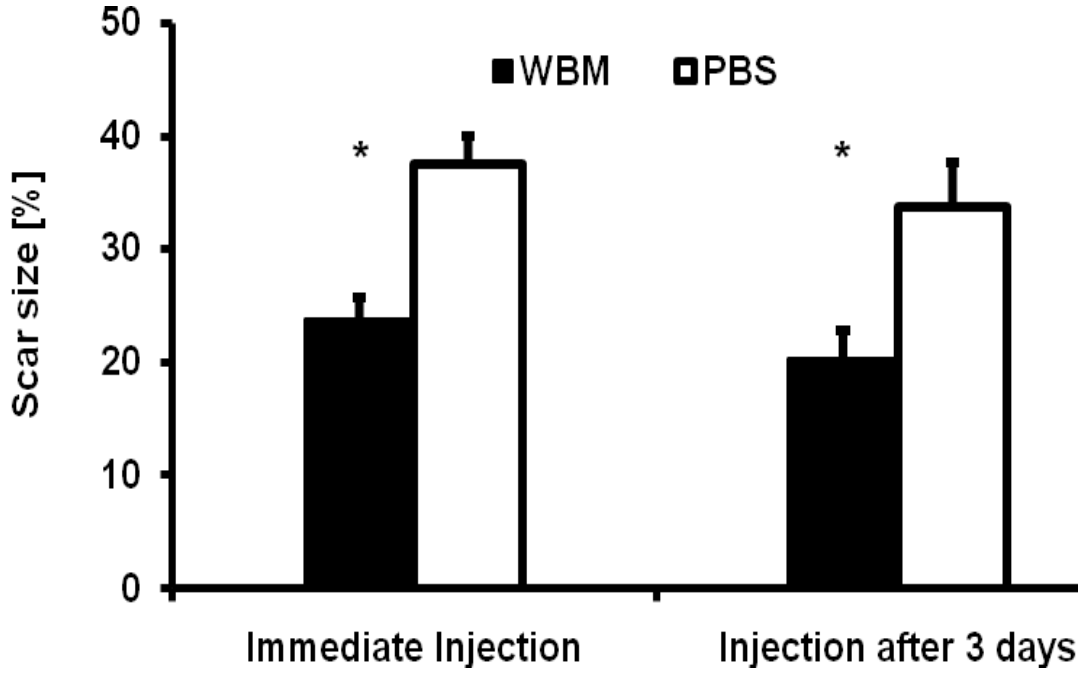

***Figure 9**: Planimetric analysis of scar area as percentage of the total left ventricular area after WBM injection as compared to the PBS injection groups; * , p<0,05.*

3.5 Course of cellular events during myocardial remodeling

3.5.1 Macrophage infiltration in reperfused infarction

The macrophage density was calculated based on F4/80s-staining (Figure 10) and showed significantly more positive cells in the whole hearts of both WBM-injected groups when compared with PBS groups after 7 days of reperfusion (Figure 11). The differential evaluation between ischemic anterior left ventricular wall and non-ischemic septum showed only a low cell influx into non-infarcted area (Figure 12).

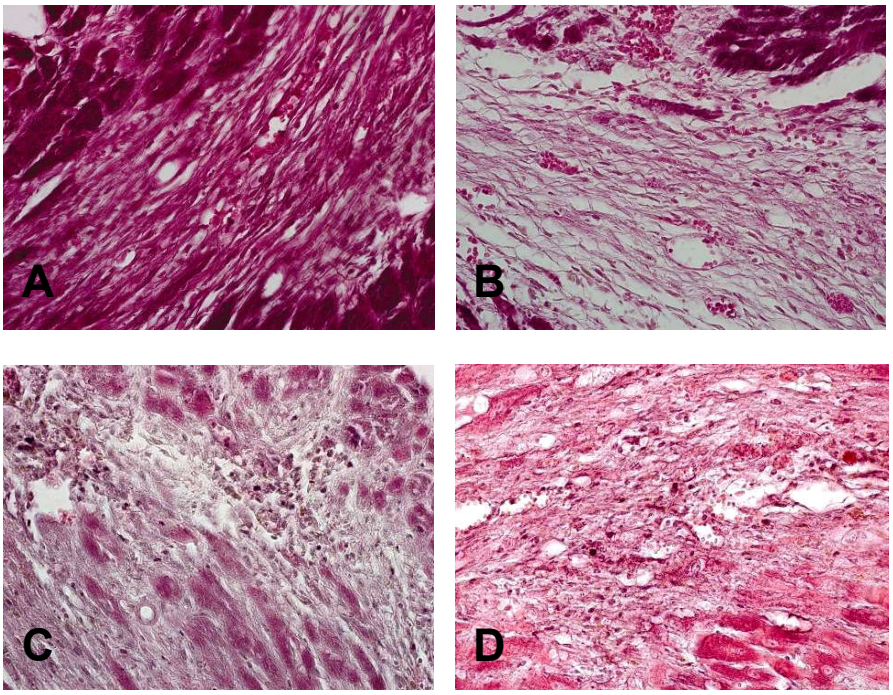

***Figure 10**: Macrophage staining using F4/80 antibody after 7 days of reperfusion. Representative slides of A) immediate and B) PBS injection after 3 days of reperfusion show lower macrophage density than in C) immediate and D) WBM injection after 3 days of reperfusion. (Magnification, 400X)*

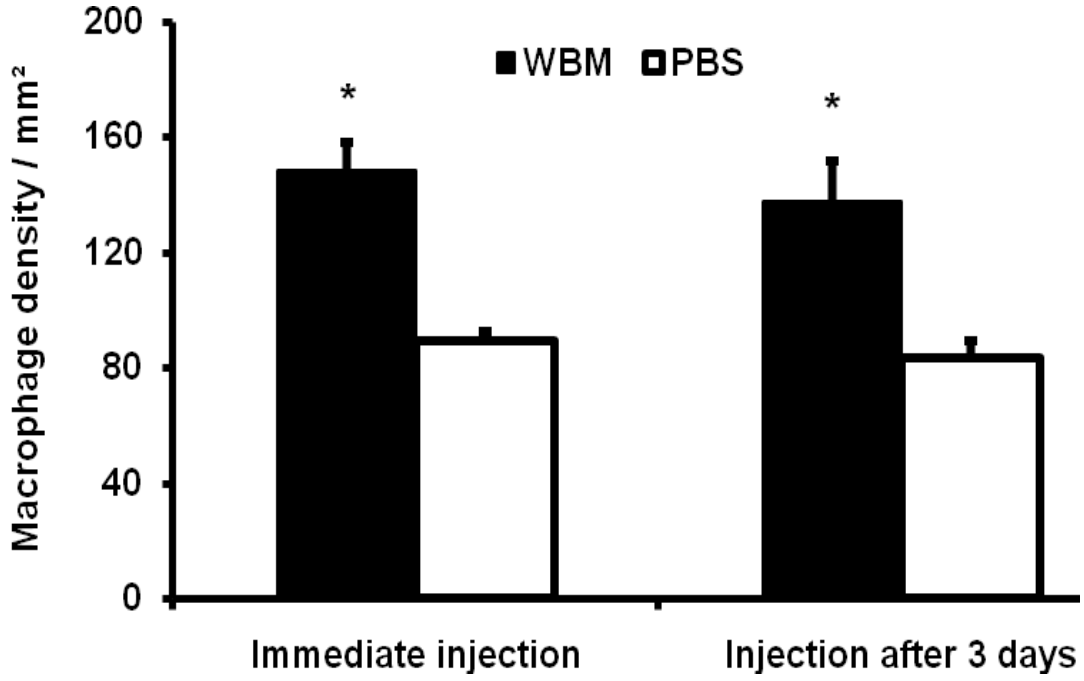

Figure 11: *Total macrophage density after 7 days of reperfusion in WBM and PBS injected hearts;* p< 0,001.*

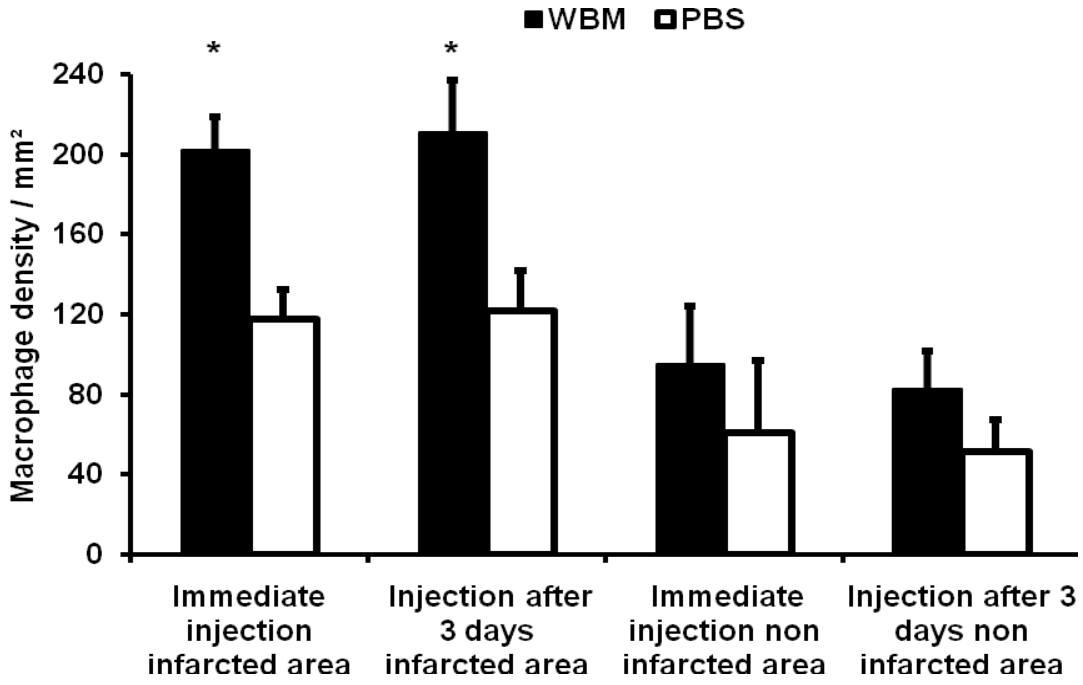

Figure 12: *Macrophage density differentiation between infarcted and non-infarcted myocardium after 7 days of reperfusion in WBM and PBS injected hearts; * p< 0,001.*

The macrophage density after 28 days of reperfusion revealed a persistent infiltration of WBM injected groups suggesting an active interstitial remodeling at this time point (Figures 13, 14). Again, the septum of all groups was not affected by macrophage influx (Figure 15).

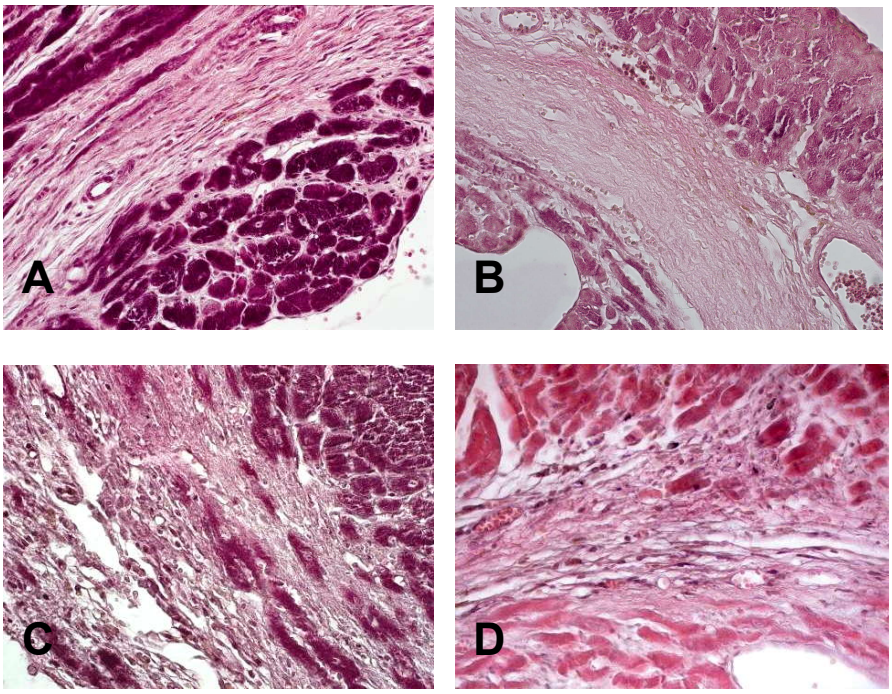

***Figure 13**: Macrophage staining using F4/80 antibody after 28 days of reperfusion. Representative slides of A) immediate and B) PBS injection after 3 days of reperfusion reveal only scattered macrophages in the scar, while C) immediate and D) WBM injection after 3 days of reperfusion led to a persistent macrophage infiltration at this time point. (Magnification, 400X)*

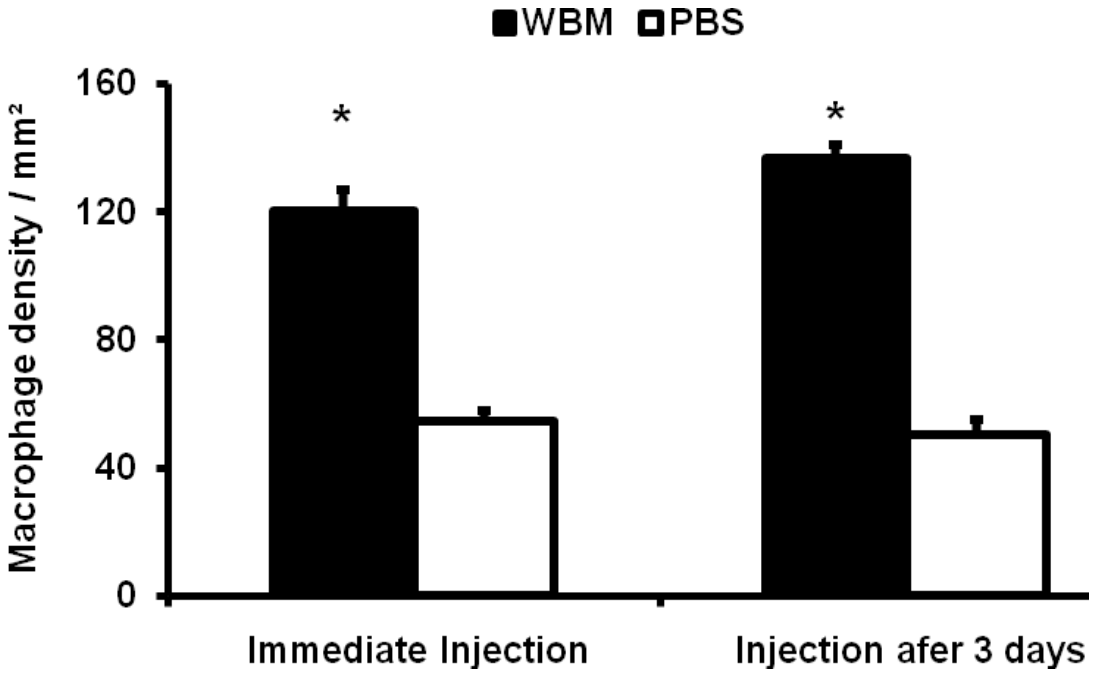

Figure 14: *Total macrophage density after 28 days of reperfusion in WBM and PBS injected hearts; *, p< 0,001.*

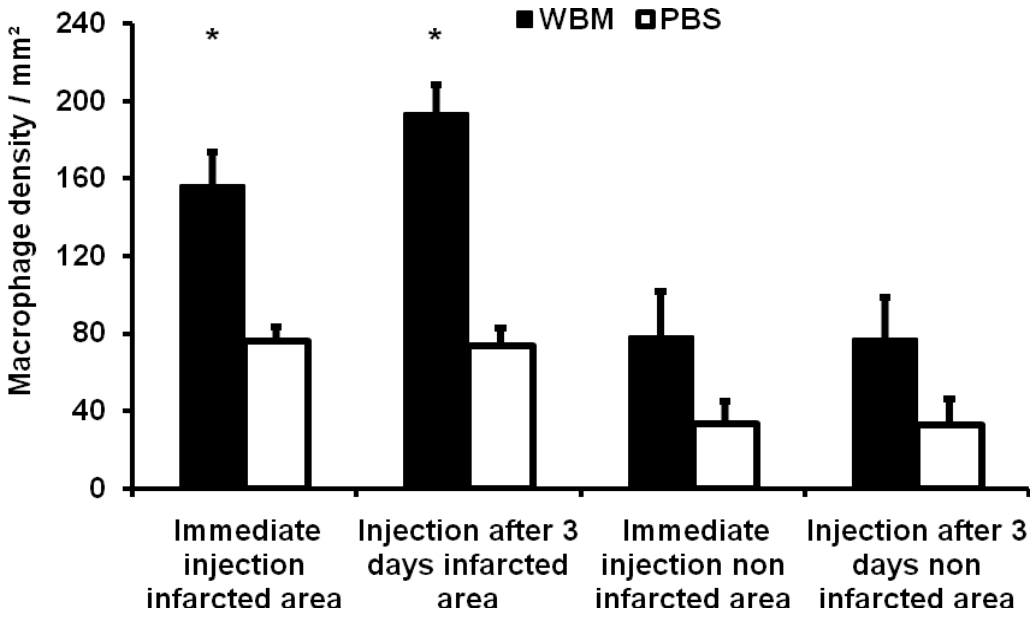

Figure 15: *Macrophage density differentiation between infarcted and non-infarcted myocardium after 28 days of reperfusion in WBM and PBS injected heart; *, p< 0,00*

3.5.2 Active interstitial remodeling and neovascularization of the scar

In order to further investigate the active interstitial remodeling after 28 days of reperfusion in WBM injected hearts the myofibroblasts were stained with α-smac. Comparable to the above mentioned findings there were only a few α-smac-positive cells in the PBS injected groups after 7 days reperfusion further supporting the rapid scar formation findings in these groups (Figure 16 A, B). In contrast, the WBM injection groups showed numerous myofibroblasts in the scar area at this time point indicating active interstitial remodeling (Figure 16 C, D).

After 28 days of reperfusion the α-smac staining was restricted to pericyte coated vessels in both PBS and WBM injection groups (Figure 17). Since the WBM injected groups appeared to have more vessels in the scar, a blood vessel count was performed for small (< 20 µm) and large (>20 µm) blood vessels in the whole heart (figure 18). The WBM injection led to a comparable blood vessel density between in both groups, which was significantly higher than in the PBS injected groups. The large vessel density showed no difference between the groups.

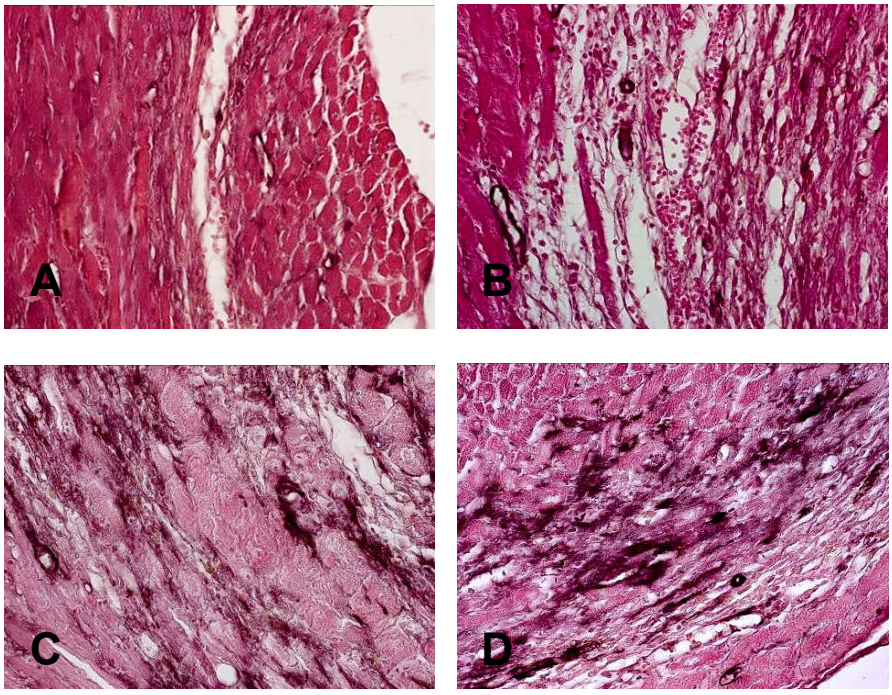

Figure 16: *Myofibroblast staining using α-smooth muscle actin (α-smac) antibody after 7 days of reperfusion. A) Immediate and B) PBS injection after 3 days specimen show only few positive*

cells, while both slides from C) immediate and D) WBM injection after 3 days contain numerous myofibroblasts indicating active interstitial remodeling. (Magnification, 100X)

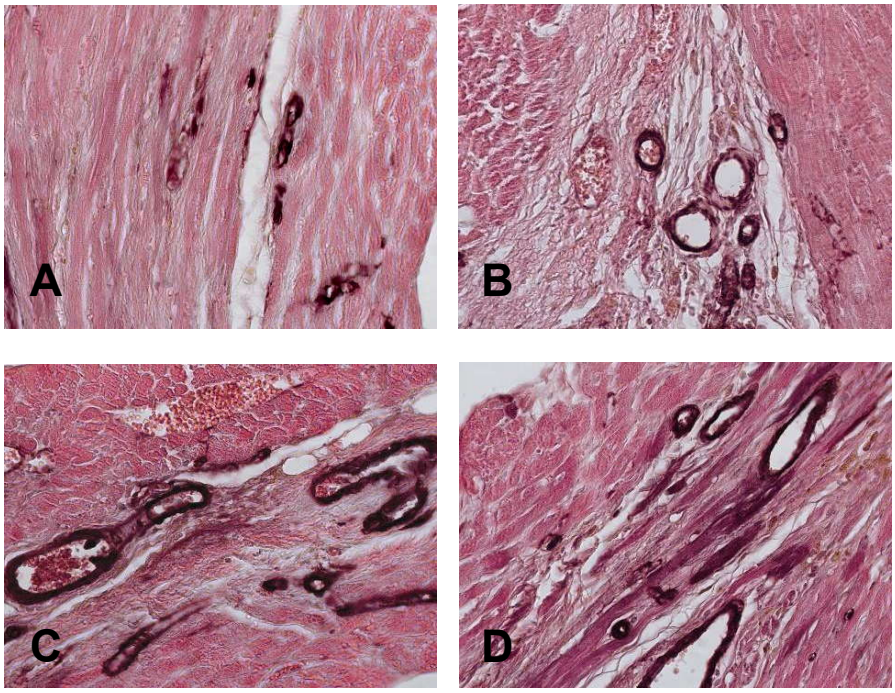

Figure 17*: α-smooth muscle actin staining after 28 days of reperfusion. While all groups show no myofibroblasts at this time point, these representative slides of A) immediate and B) PBS injection after 3 days of reperfusion show less blood vessels than those of C) immediate and D) WBM injection after 3 days of reperfusion. (Magnification, 400X)*

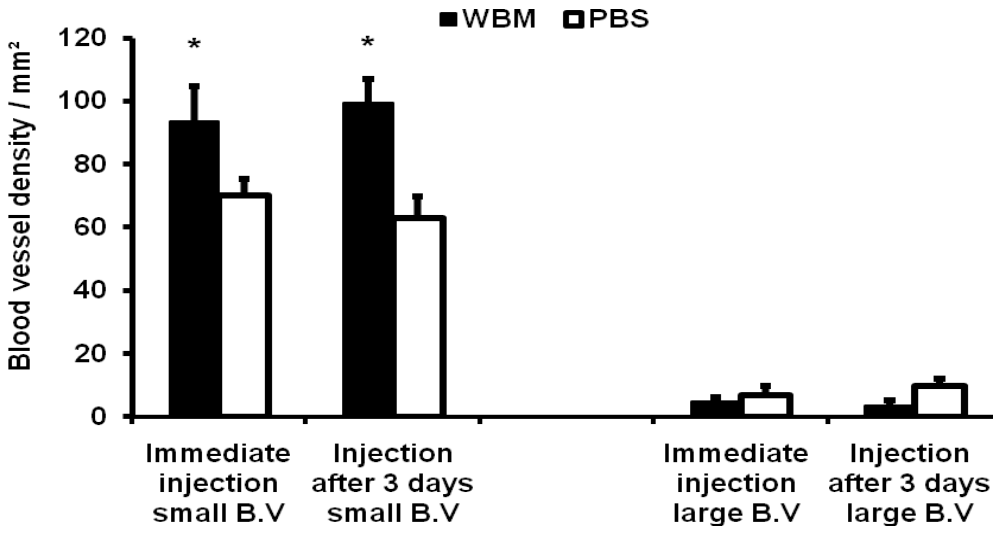

Figure 18: *Quantitative analysis of blood vessels based on α–smac staining after 28 days of reperfusion. Small blood vessels were defined by diameter <20 µm, large blood vessels by > 20 µm; *, p<0,05.*

3.6 Characteristics and differentiation of injected cells in myocardium

Loop fluorescent microscopy revealed the homing of injected GFP-positive WBM cells in the mice. While some GFP-positive cells were found in the heart, most of the cells were homing to the spleen and few of them in the liver (Figure 19). Interestingly, a very few GFP-positive cells were found in the spleen even after 28 days of reperfusion in both groups, suggesting their persistence or even a possible recirculation in the body.

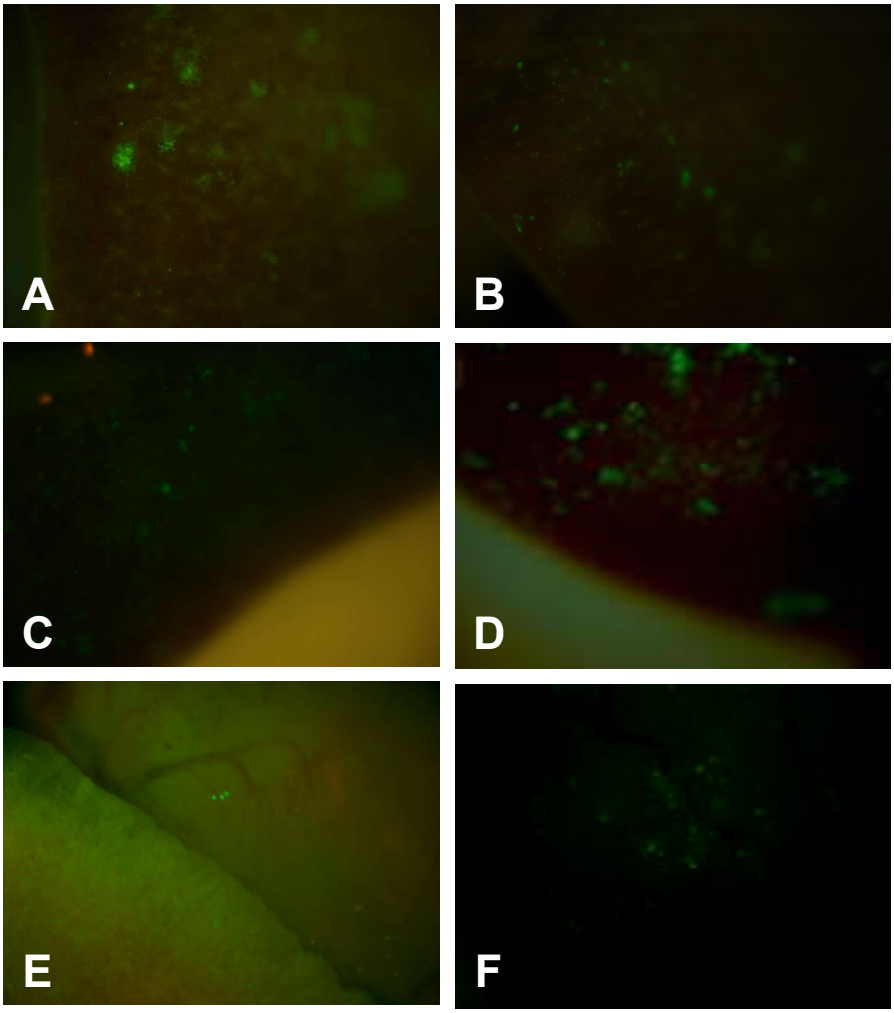

Figure 19: *GFP^+ cells in spleen and heart after WBM injection visualized using loop fluorescent microscopy. A) Immediate and B) WBM injection after 3 days lead to maximal accumulation of GFP+ cells in the spleen after 7 days of reperfusion. After 28 days of reperfusion there were still significant numbers of cells in the spleen of mice after C) immediate) and D) WBM injection after 3 days. The heart shows after 7 days of reperfusion only few GFP+ cells in E) immediate and F) WBM injection after 3 days group (Magnification of figure A,B,C,D are 50X and figure E,F are 8X)*

In order to characterize the GFP+ cells in the heart a fluorescent immunostaining was performed. Morphologically, these cells were small and either round or elongated in shape and none of them were positive for either troponin T or α-smac (Figure 20). Nearly 90 % of GFP+ cells were concomitantly positive for panhematopoietic cell surface antigen CD 45 (Figure 21). The further differentiation of these cells revealed only a few of them being positive for monocyt/ macrophage specific marker MAC 2 (Figure 22).

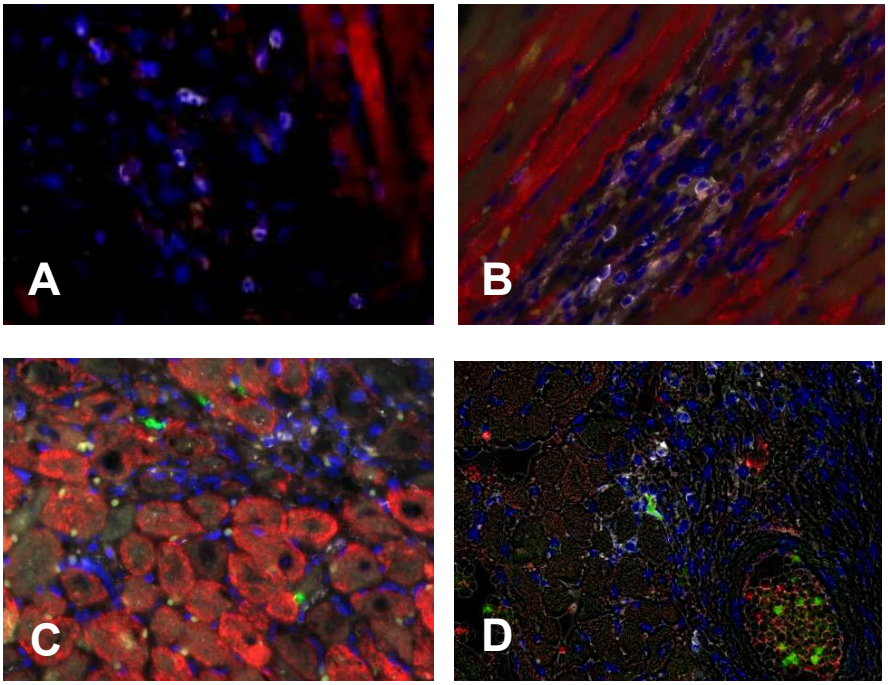

***Figure 20**: Characterization of GFP$^+$ cells in infarcted myocardium after 7 days of reperfusion I. A) Immediate and B) PBS injection after 3 days of reperfusion show only a few CD 45-positive cells (white) in the scar; troponin T red. Representative slides of C) immediate and D) WBM injection after 3 days of reperfusion show only a few GFP+ cells (green) in the infarction, which are mostly CD 45 positive. (Magnification, 400X)*

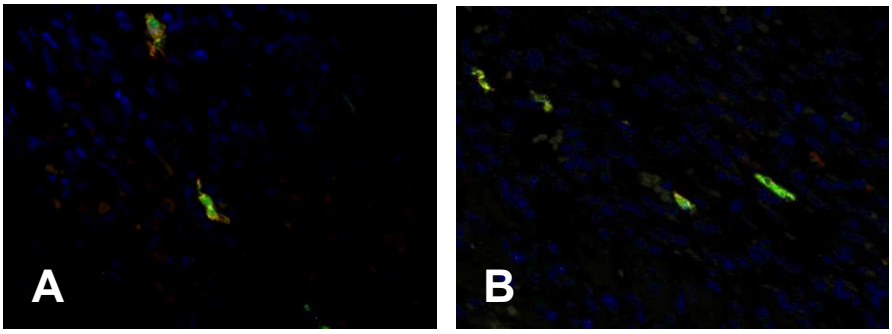

***Figure 21**: Characterization of GFP$^+$ cells in infarcted myocardium after 7 days of reperfusion II. A) Immediate and B) WBM injection after 3 days of reperfusion were both associated with only a few GFP+ cells (green) in the infarction, which were in almost 90 % simultaneously positive for pan hematopoietic CD 45 (red). (Magnification 400X)*

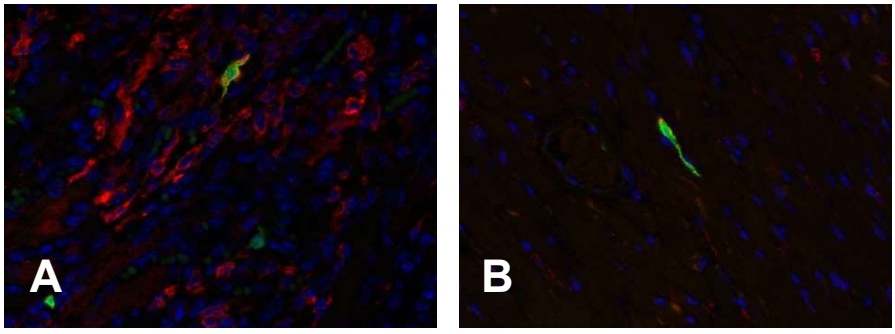

***Figure 22**: Characterization of GFP$^+$ cells in infarcted myocardium after 7 days of reperfusion III. Only few of GFP+ cells in heart after A) immediate and B) WBM injection after 3 days of reperfusion were simultaneously positive for monocyte/macrophage related marker MAC 2 (red). (Magnification, 400X)*

Differential quantitative analysis showed a rather low total number of GFP+ cells in the whole heart (Figure 23). Interestingly, the immediate WBM injection led to significantly more cells in the infarcted area and border zone after 7 days of reperfusion than the injection after 3 days of reperfusion, suggesting a probable difference in the local environment, e.g. stage of inflammatory reaction or active interstitial remodeling. GFP $^{+}$ cells in WBM injection immediately and after 3 days of infarction and 7 days of reperfusion which mainly found in the infarcted area and some in the border zone.

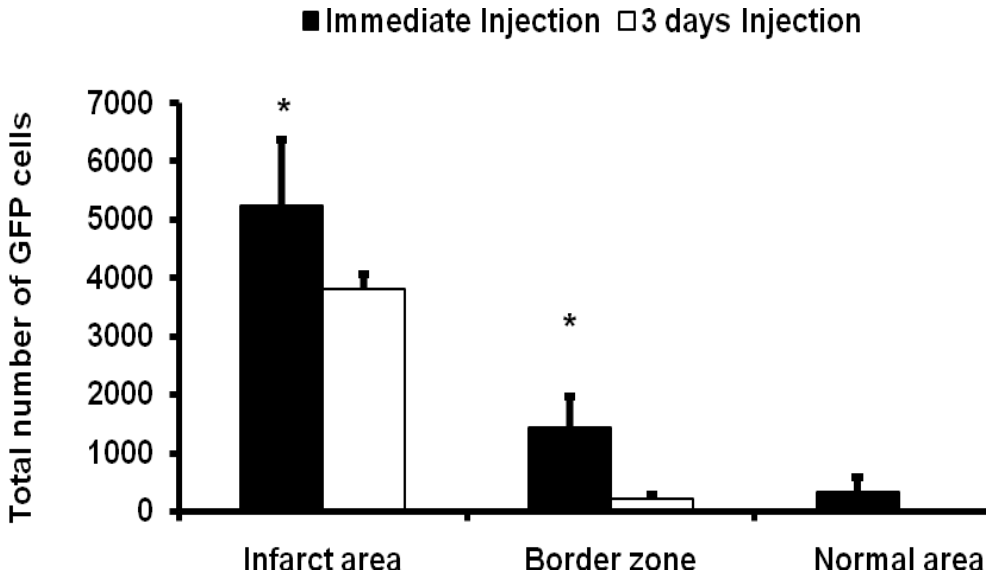

=

***Figure 23**: Total GFP^{+} cell count in the whole heart is differentiated by homing into infarcted area, border zone and non-ischemic normal area;*, p<0,05.*

3.7 Impact of WBM injection on inflammatory and remodeling mediators

In order to better understand the impact of WBM injection on the molecular events in reperfused myocardium mRNA expression of a number of inflammatory mediators and remodeling related factors were investigated after 7 days of reperfusion using Taqman qRT-PCR. These specific mediators were chosen as representative members of their groups based on findings from several previous studies in this model.

3.7.1 Cytokines:

3.7.1.1 Tumor necrosis factor α

The immediate WBM injection did not affect the expression of proinflammatory TNF-α after 7 days of reperfusion and showed comparable expression level as in the sham operated or PBS control group (Figure 24). The WBM injection after 3 days of reperfusion led to persistent, significantly higher induction of TNF-α at this time point.

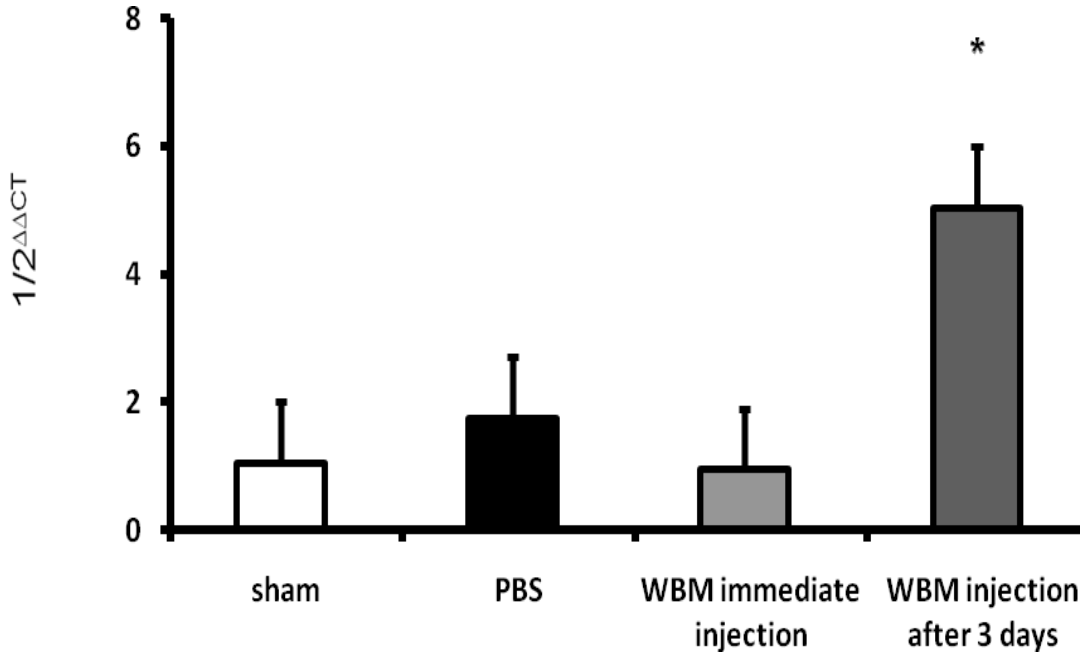

***Figure 24**: TNF-α mRNA expression in myocardial infarction after 7 days of reperfusion *, p<0,05 vs. PBS and vs. WBM immediate injection.*

*3.7.1.2 Interleukin 1*β

The WBM injection had no significant influence on the expression of proinflammatory IL-1β when compared to the control hearts (Figure 25). When compared with sham operated mice there is persistently higher induction of it despite the resolution of the inflammatory response in the PBS mice.

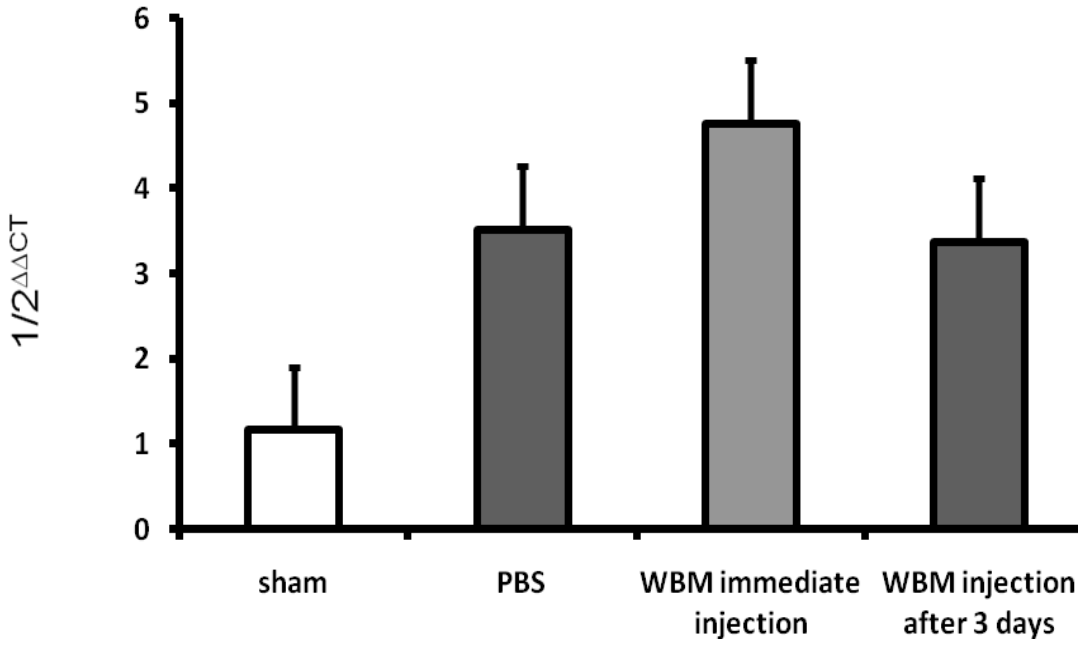

Figure 25: *IL-1*β *mRNA expression in myocardial infarction after 7 days of reperfusion.*

3.7.1.3 Interleukin 10

The mRNA expression of IL-10, as a representative anti-inflammatory cytokine, showed no significant difference between the groups (Figure 26). Still, its expression is relatively higher in the WBM injection after 3 days of reperfusion group, suggesting a relative induction in order to control the proinflammatory TNF-α.

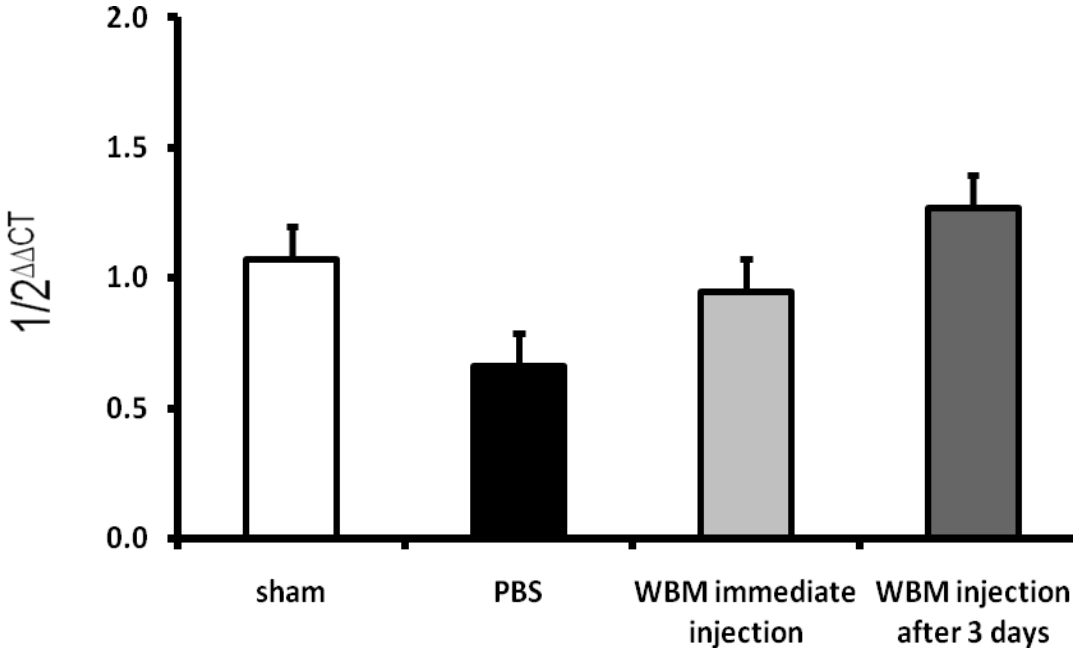

Figure 26*: mRNA expression of IL-10 in myocardial infarction after 7 days of reperfusion.*

3.7.2 Chemokines:

3.7.2.1 CC-chemokine ligand 2

CCL 2 as the most potent chemoattractant for monocytes and macrophages showed comparable expression between the PBS and WBM injected groups (Figure 27). This level was again higher that in the sham mice suggesting its role in later stages of remodeling.

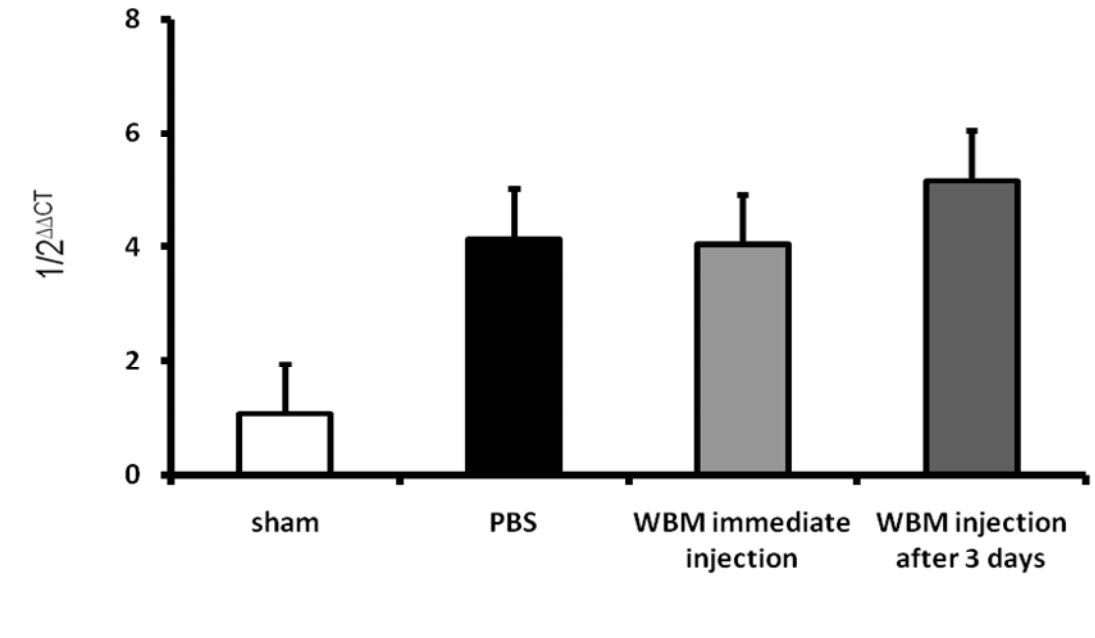

Figure 27*: CCL 2 mRNA expression in myocardial infarction after 7 days of reperfusion.*

3.7.2.2 CC-chemokine ligand 4

The CCL 4, as another prominent chemoattractant, showed comparable expression between the PBS and WBM immediately injected mice (Figure 28). In contrast to CCL 2, there was a significant induction of CCL 4 in the WBM injection after 3 days of reperfusion group supporting the evidence of prolonged inflammatory response in these mice.

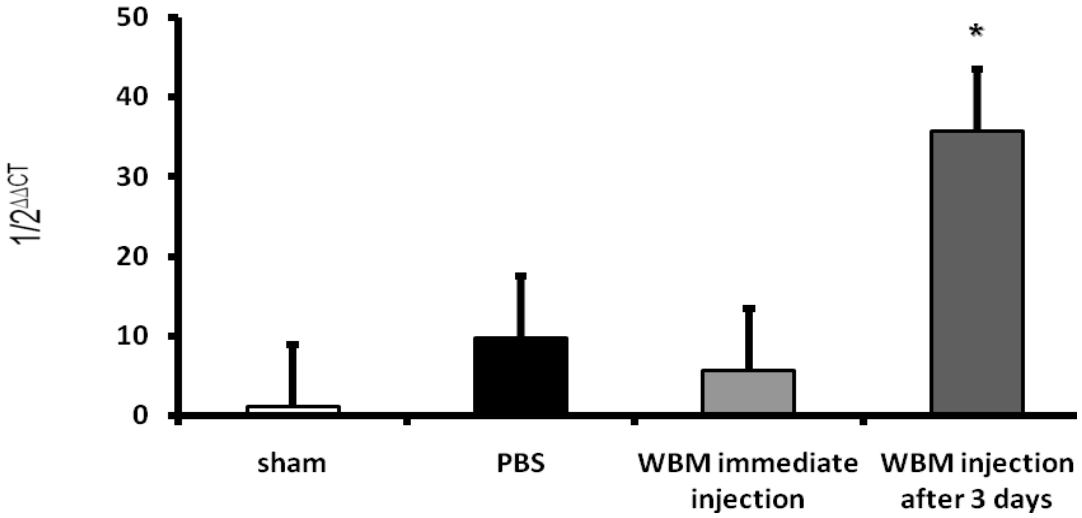

***Figure 28**: CCL 4 mRNA expression in myocardial infarction after 7 days of reperfusion; *, p<0,05 vs. PBS and vs. WBM immediate injection.*

3.7.3 Remodeling related cytokines:

3.7.3.1 Osteopontin

The mRNA expression of macrophage maturation marker and extracellular matrix glycoprotein osteopontin we showed no difference between the groups (Figure 29).

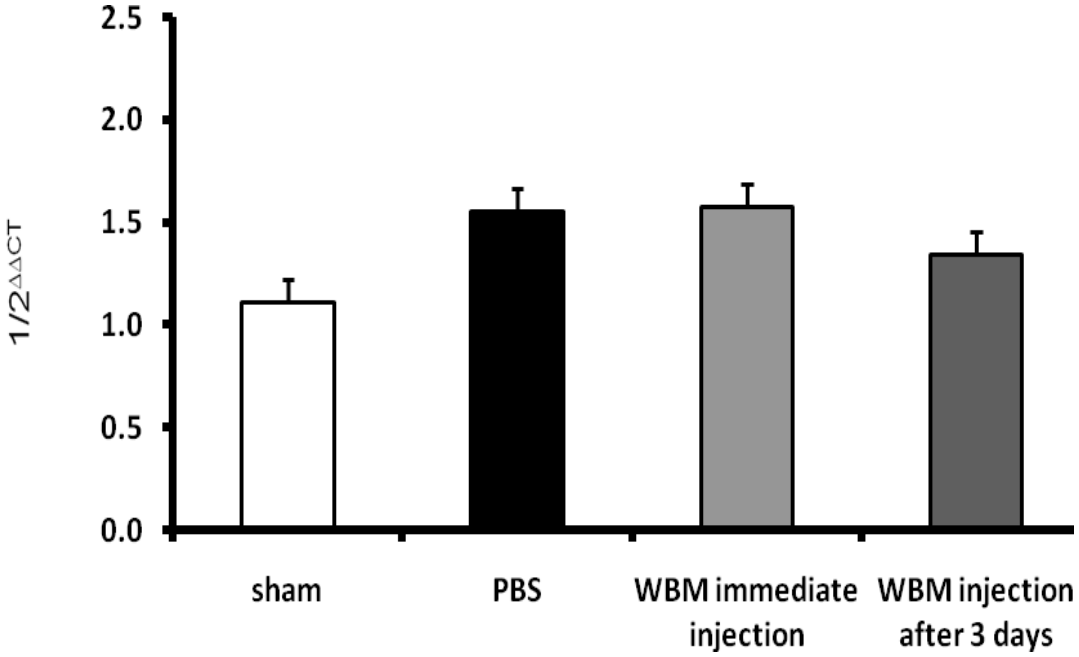

Figure 29: *Osteopontin 1 mRNA expression in myocardial infarction after 7 days of reperfusion.*

3.7.3.2 Transforming Growth Factor β isoforms

The isoforms of TGF-β 1, 2 and 3 are associated with different stages of extracellular matrix remodeling. The profibrotic TGF-β1 showed slight induction in PBS and immediate WBM injection group when compared to the sham operated mice (Figure 30). The WBM injection after 3 days led to a significant induction of TGF-b1 mRNA expression when compared to the PBS and immediate injection group.

The predominantly antifibrotic acting TGF-β2 showed significantly higher induction in PBS group than in the both WBM injected groups (Figure 31). Still both WBM injected groups showed a strong induction of TGF-β2 when compared to the sham operated mice.

TGF-β3, as mostly profibrotic mediator showed similar pattern to the TGF-β1 with significantly higher induction in the WBM injection after 3 days of reperfusion group than in the PBS or immediate WBM injected hearts (Figure 32).

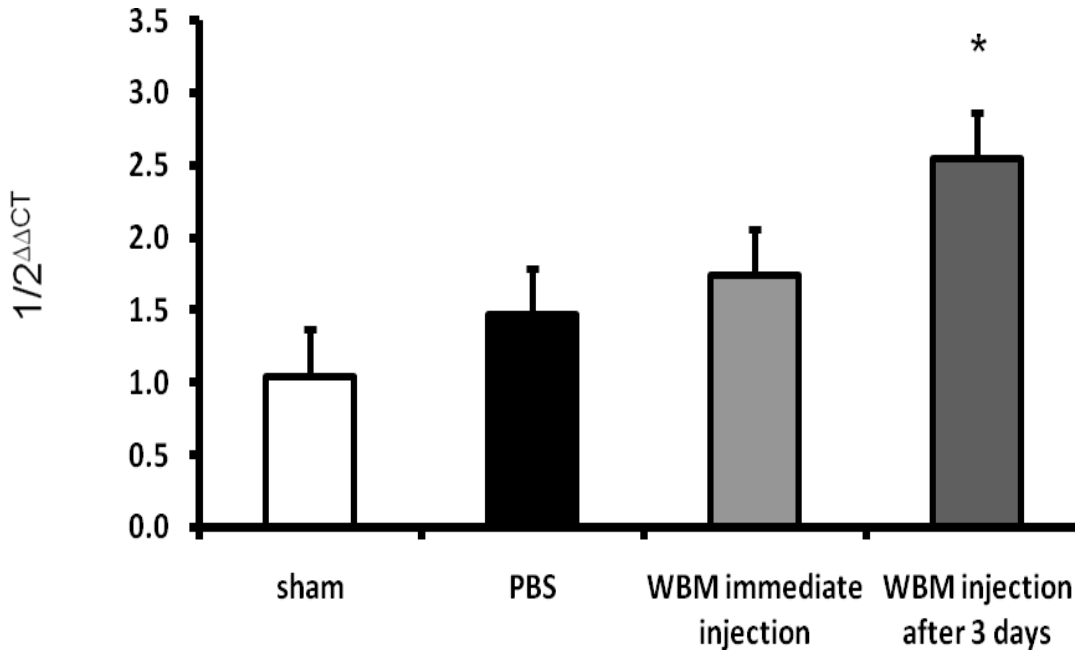

***Figure 30**: mRNA expression of TGF-β1 in myocardial infarction after 7 days reperfusion; *, p<0,05 vs. .PBS and vs. WBM immediate injection.*

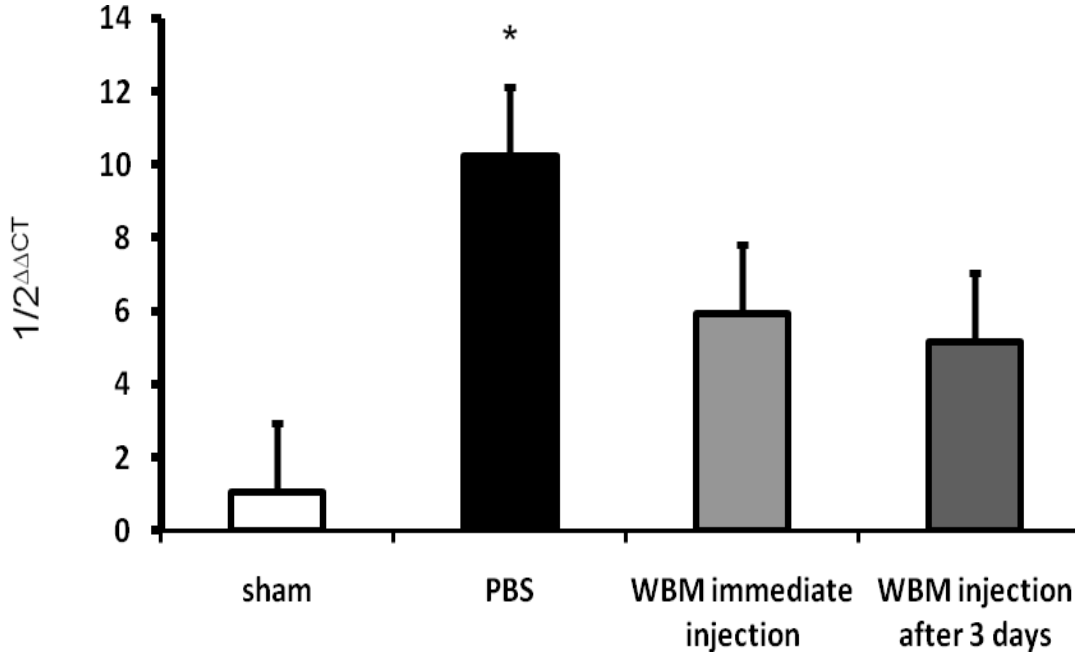

***Figure 31**: mRNA expression of TGF-β2 in myocardial infarction after 7 days of reperfusion; *, p<0,05 vs. PBS and vs. WBM immediate injection.*

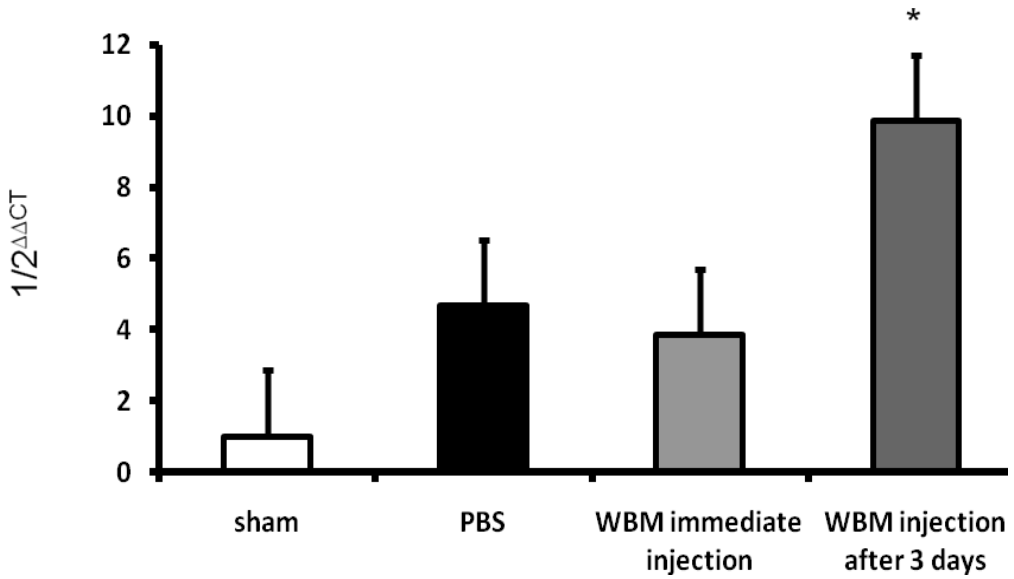

***Figure 32**: mRNA expression of TGF-β3 in myocardial infarction after 7 days of reperfusion; *, p<0,05 vs. PBS and vs. WBM immediate injection.*

4 Discussion

Cardiovascular diseases and especially the coronary artery disease represent a major cause of death in the last few decades, with a constantly growing incidence worldwide. The therapeutic options are mostly restricted to the manifested disease, including the therapy of concomitant diseases of the metabolic syndrome (Kloner et al., 1998). The narrowing of the coronary vessels leads to classical symptoms and need for revascularization in order to preserve the myocardial function and prevent myocardial infarction. In event of myocardial infarction an early reperfusion is the treatment of choice in order to limit the extent of the tissue damage and thus influence the long-term prognosis. Since infarction is associated with a number of complications and significant mortality with only a few therapeutical options beside revascularization (reperfusion) are available in order to limit its extent, there is a great need for novel therapies aiming for better myocardial remodeling or tissue regeneration. The cellular therapy options have emerged in the last few years with a potential to positively influence this field, but the limited understanding of the complex pathomechanisms and cellular interactions leads to a necessity for further studies (Amber D et al., 2006).

Coronary artery occlusion is associated with cardiomyocyte death due to necrosis or apoptosis and triggers a more or less intense inflammatory reaction, which depends on the vessel reperfusion. At this early stage of myocardial repair a superbly orchestrated interaction of cells, cytokines, growth factors and extracellular matrix proteins is found (Cleutjens JP et al., 1995; Frangogiannis NG et al., 1998; Willems IE et al., 1994; Richard V et al., 1995; Mehta JL et al., 1999). One of the early features of inflammatory response is immigration and differentiation of macrophages, which remove necrotic cardiomyocytes and mediate together with myofibroblasts the formation of granulation tissue. In addition, chemotactic factors such as the chemokines CCL2, CCL3 and CCL4 are highly induced in mouse model of myocardial infarction and seem to critically regulate inflammatory cell recruitment (Dewald et al., 2004). This transient induction of cytokines, chemokines and other adhesion molecules leads after 24 hours of reperfusion to an induction of remodeling related mediators and is followed by deposition of collagen and subsequent myocardial scar formation. The scar size is clinically the major long-term determinant influencing cardiac dysfunction, morphometric abnormalities, incidence of pathological events and mortality (Peffer et al .1979; Peffer and Braunwald 1990).

Development of heart failure after infarction is closely related to alterations in left ventricular structure. Myocardial geometry changes after infarction are leading to hypertrophy of remote myocardium and expansion of the myocardial border zone and scar. All of these events are summarized as post infarct remodeling (Yang et al .2002; Jakson BM et al .2002; 2005).

Many investigators aim to reverse the myocardial remodeling and focus to decrease the scar size. One of these approaches is to repair the myocardial tissues using stem cells. Bone marrow contains multipotent adult stem cells that show a high capacity for differentiation. Many experimental studies have shown that BMCs are associated with regeneration of infracted myocardium through myogenesis or angiogenesis, thus leading to amelioration of cardiac function in mice and pigs (Orlic D, et al., 2001; Tomita S et al., 2002). The regenerative properties of bone marrow stem cells have also been found advantageous in the attempt to restore myocardial function in patients with acute myocardial infarction (Strauer BE et al., 2002; Wollert KC, et al., 2004). Despite of these promising results there are also experimental data showing potential negative effects of bone marrow transplantation and especially the mesenchymal stem cells in murine infarction (Breitbach et al., 2007).

A critical step for the clinical success of stem cell–based therapy for myocardial repair is an efficient method for cell delivery. Intravenous delivery of bone marrow–derived stem cells is simple and minimally invasive in nature, which could be literally carried out in emergency rooms and primary care hospitals without the need for surgical intervention or cardiac catheterization, which is normally performed during bone marrow transplantation to patients recovering from myocardial infarction. Furthermore, it may be applicable to patients with diffuse myocardial disease such as idiopathic dilated cardiomyopathy.

Based on these findings and our combined experimental expertise we investigated the role of whole bone marrow injection in a murine model of reperfused myocardial infarction aiming at a better understanding of remodeling process and long-term function.

In our study, the I.V injection of WBM after reperfusion of myocardial infarction showed a significant functional improvement after 28 days when compared to the PBS-injected control hearts. One possible explanation for this finding is a significantly smaller scar size with a better preservation of the ventricular geometry in WBM-injected hearts. This explanation must be accompanied by a word of caution due to a basic problem in our experimental model, where there may be a variation of the coronary anatomy and thus area at risk may strongly influence the scar size. Still, in another study Virag and Murry found an even more pronounced decline in infarct

size after 4 weeks (Virag JI et al., 2003), thus supporting our interpretation. On the other hand, the WBM injection is associated with cellular paracrine effects, which themselves can further facilitate the myocardial repair and scar size limitation. We tried to dissect the course of these events by investigating cellular and molecular events and mediators involved.

Our functional data are comparable with other studies, where WBM injection into myocardium or coronary arteries led to cardiac function improvement after myocardial infarction. Among others, Chen J et al reported that systemic administration of bone marrow stromal cells improves function and angiogenesis in the rat model, (Chen J et al 2001; 2003). Chen SL et al demonstrated that bone marrow mesenchymal stem cells significantly improved left ventricular function in patient with acute myocardial infarction (Chen SL et al ;2004).

In a different model of permanent coronary artery occlusion we demonstrated that neither direct injection nor cytokine-induced mobilization of BM cells were able to reduce scar formation and/or improve left ventricular function after 4 weeks (Kolossov et al., 2006). Therefore, the local events and the microenvironment in the damaged myocardium strongly influence the course of myocardial remodeling and scar formation.

This study showed important insights into cellular events during remodeling of the reperfused infarction. The regular course of remodeling in this model includes development of granulation tissue after 3 days and formation of a compacted scar tissue after 7 days of reperfusion (Dewald et al., 2004). The immediate WBM injection led to a prolonged cellular infiltration and development of granulation tissue after 7 days. The WBM injection after 3 days reperfusion showed a comparable cellularity in the infarction and also a lack of scar formation at the same time point. Still, all four groups showed a compacted myocardial scar after 28 days reperfusion, suggesting that WBM injection led to a modulation of the remodelling process with postponed scar formation resulting in a persistence of a few cardiomyocytes within the scar area. Whether these cardiomyocytes survived the infarction or emerged from some progenitor cells remained unclear, since none of cardiomyocytes evaluated was positive for GFP. Still, the functional data suggest that this was beneficial, even though this pathology may be associated with clinically relevant complications, e.g. arrhythmias or ventricular rupture, which are rare in this model. The further evaluation of cellular events revealed a significantly higher macrophage density in WBM injected groups after 7 days of reperfusion, which may well be attributable to the paracrine effects of the injected cells. Significantly higher macrophage density was even found after 28 days reperfusion, thus giving further support to possible paracrine effects of WBM cells. The α-smac

positive myofibroblasts accompanied the macrophages after 7 days reperfusion in WBM groups in contrast to their absence in the control hearts, thus further supporting this explanation. Nevertheless, we found absence of myofibroblasts after 28 days reperfusion, but a significant increase in small arterioles and thus better vascularisation in WBM-treated groups, which could also contribute to the better functional results. Neovascularization of the healing myocardium is also crucial determinant of cardiac repair. The angiogenesis relies on capillaries sprouting from pre-existing blood vessels, as well as on the migration and incorporation of the bone marrow derived endothelial progenitor cells (Asahara T et al., 1999). The mediators responsible for the vessel formation have not been fully elucidated, however the contribution of a wide variety of cytokines and growth factors has been suggested (Schaper W, et al., 1996; Kersten JR. et al., 1999).

The WBM cell characterization revealed very interesting insights into cell fate and homing after I.V delivery. GFP^+ WBM cells engrafted in both infarction and border zone irrespectively of the injection time point. The immediate WBM injection was even associated with a few GFP^+ cells in remote, non-infarcted area areas. While the total number of the cells in the whole heart after 7 days reperfusion was very low, we still found significantly more cells in the immediately injected group, which may be explained by preferential microenvironment features and mediators in this group. The presence of GFP^+ cells after 7 days of reperfusion can be explained by either persistence in the infarcted heart or an even more probable event of recirculation of injected cells from other organs. The low number of cells, which were incorporated into the heart, is in line with reports on human sex-mismatched transplanted cells where less than 1 % of the infused cells were found in the heart (Muller et al., 2002, Laflamme et al., 2002), thus suggesting a WBM cells homing to other tissues, e.g. spleen and liver. In our study, we found a low persistence of the injected WBM cells in the hearts and numerous GFP+ cells in the spleen after 28 days reperfusion. So, it is probable that the most of our injected cells are homing to the spleen, which may serve as a reservoir for a constant release on demand. The constant release from the spleen and the presence of the cells in the infarction may be related to a continuous, probably low level chemotactic signalling from the active interstitial remodeling, which can be assumed based on higher macrophage density after 28 days.

Homing of bone marrow cells to the infarcted myocardium after intravenous injection has been compared in two studies (Barbash IM et al 2003; Hou D, et al., 2005). In one of these studies, MSCs were used and their homing to the infarcted myocardium seemed to be limited by lung

entrapment after I.V injection due to their large size (Barbash IM et al 2003). In the other study, the homing efficacy to the infarcted myocardium might have been limited by subsiding homing signals from the infarcted tissue, since the cells were administered 6 days after infarction (Hou D,et al .,2005), Another study used injection of bone marrow mononuclear cells via tail vein and showed also preferential homing with higher number of cells in the heart than in controls after one week (Ahmed Y.Sheikh et al., 2007).

Further characterization of our incorporated GFP+ cells showed that after 7 days reperfusion the vast majority of the cells were CD45-positive leukocytes, whereas none of the cells stained positive for cardiomyocyte markers. Further differentiation of these inflammatory cells identified primarily macrophages, suggesting beneficial effects of these cells on prolonged active remodeling. Comparable findings were also described by other groups (Virag et al., 2003).

In our study, we demonstrated that intravenous injections of WBM cells led to engraftment in ischemic myocardium. The restoration of circulation into infracted area gave the cells not only a better access to the damaged tissue, but also led to a stronger exposure to chemotactic mediators, which are released from the ischemic myocardium during reperfusion. There is a fair evidence that ischemic injury to the heart can lead to increased homing of bone marrow stem cells to the injured tissue (Orlic D et al., 2002). Many studies suggested that the ischemic tissue may express specific receptors or ligands to facilitate trafficking, adhesion and infiltration of WBM cells to ischemic sites, but only a few specific mediators were described by now.

In order to better interpret our functional and morphological data, we measured expression of several inflammatory and remodeling-related mediators after 7 days reperfusion. An early expression of several proinflammatory mediators has been described after reperfusion of myocardial infarction in several animal models (Frangogiannis et al., 2000**)**.

Our previous study showed only a transient induction of proinflammatory cytokines and chemokines in our model of reperfused infarction (Dewald et al, 2004). While the immediate injection of WBM cells led to a comparable level of proinflammatory cytokine TNF-α mRNA expression, the WBM injection after 3 days led to a significantly higher expression of it after 7 days reperfusion. At the same time, there was a comparable expression of another proinflammatory cytokine IL-1β between the groups. The most notable finding was a relative induction of expression of anti-inflammatory cytokine IL-10 in the WBM 3 days injection group to control the control the proinflammatory TNF-α, whereas the other groups show a strong induction of this important factor for resolution of inflammation. These findings demonstrate for

the first time, that the immediate injection of the WBM cells allows a normal resolution of inflammation, even with a prolonged cellular response after 7 days reperfusion. On the other hand, the WBM injection after 3 days reperfusion leads to a strong proinflammatory burst impacting the course of remodeling at a time point where the inflammation has already being resolved. Despite of the beneficial functional data in this model, the application of the WBM cells at this time point may induce severe adverse effects in large animal models, and should therefore be carefully studied further.

The mRNA-expression of chemotactic mediators CCL2 and CCL4 showed similar results as the cytokines. Both chemokines showed higher expression after 7 days reperfusion in WBM injection after 3 days group, thus further supporting the sustained proinflammatory environment. At the same time, these mediators are responsible for macrophage attraction and differentiation in the infarction. In addition, CCL2 can interact with myofibroblasts and contribute to collagen production, thus giving additional support to the presence of active interstitial remodeling process.

The persistent macrophage influx and activity in the infracted heart after WBM cell injection after 3 days is also supported by the lack of expression of osteopontin. This glycoprotein is not only a macrophage maturation marker, but also found in the extracellular matrix during tissue remodeling (Frangogiannis et al., 2000), and its lack of expression further suggests a significant impact of our cellular therapy on the myocardial remodeling. Another important marker of myocardial remodeling is the TGF-β with its three isoforms. TGFβ expression is important in remodeling of myocardial infarction due to its ability to enhance collagen synthesis, angiogenesis and compensatory myocardial hypertrophy. Beside its important role in regulating matrix deposition, it is critical for differentiation myofibroblasts expressing α-smooth muscle actin and other contractile elements, which are important for wound contracture (Tomasek JJ et al., 2002). The macrophages release TGF-β upon the Th2-polarisation, and this leads to differentiation of myofibroblasts and subsequent deposition of extracellular matrix and scar components (Frangogiannis et al. 2000). Our data showed a comparable occurrence of myofibroblasts between both WBM-injected groups, which was prolonged than in the controls. Interestingly, we found a stronger induction of TGF-β1 and 3 along with a lower expression of TGF-β2 in the group with WBM cell injection after 3 days, thus further supporting the manifold impact of this later cell injection on the course of myocardial remodeling. On the other hand, we found comparable level of TGF-β isoforms in immediately injected WBM group as in controls, which may lead to a

conclusion, that the most favourable microenvironment for functional improvement is achieved, when the cells are injected immediately or early after reperfusion on myocardial infarction. Other studies also showed evidence that elevated levels of TGF-β in the early phase of reperfusion are important to preserve cardiac function (Bujak M et al., 2007; Ikeuchi M et al., 2004). Since the available data on exact role of each isoform are not congruent, it is very difficult to assign a specific role of them in our experimental mode. Nevertheless, the isoforms 1 and 3 seem to represent the profibrotic response, while the isoform 2 is mostly associated with antifibrotic properties, which are very important in resolution of remodeling and formation of a stable scar.

In conclusion, our study showed promising data regarding the WBM I.V cell injection after reperfusion of myocardial infarction. The most functional benefit was achieved when cells were injected immediately after reperfusion, this was associated with prolonged formation of granulation tissue and active interstitial remodeling after 28 days of reperfusion. The WBM cell injection after 3 days of reperfusion showed also an improvement in left ventricular function, even though not being significant. This later injection led to reactivation of inflammatory response in the already formed granulation tissue and thus postponed development of a regular scar. Since the scar size was smaller in both treated groups it seems that the prolongation of remodeling in its early stages and persistence of its activity after 4 weeks are directly associated with WBM cell treatment. The higher vascular density in the WBM groups, gives additional support to these findings. The cellular characterisation provided evidence to support the process of WBM cell recirculation from the spleen and their phenotype showed predominant differentiation of cells from the monocyte-macrophage lineage. The molecular findings support additionally our histological findings, with persistent induction of proinflammatory mediators especially found in the WBM injection after 3 days group. The difference in remodeling marker expression further supported the influence of WBM cells on the remodeling process. The data presented in this study suggest a beneficial effect of WBM cells as a treatment option after myocardial infarction, but our understanding of the underlying mechanisms and cellular interaction still needs to be improved. Our data seem to be promising for a future clinical application, but before that further profound experimental and clinical studies have to be done.

5 List of figures and tables

6. Reference

1. Abbott JD, Huang Y, Liu D, Hickey R, Krause DS, Giordano FJ. Stromal cell-derived factor-1 alpha plays a critical role in stem cell recruitment to the heart after myocardial infarction. Circulation 2004; 110: 3300– 3305

2. Ahmed Y. Sheikh, Shun-Anlin, Feng Cao, Yuan Cao, Koen E.A.Van der bogt, Pauline Chu ,Ching-Pinchung ,Christroper H.Contag, Robert C.Robbins, Joseph C. Molecular imaging of bone marrow mononuclear cell homing and engraftment in ischemic myocardium. Stem cells 2007; 25: 2677-2684

3. Aikawa Y, Rohde L, Plehn J, Greaves SC, Menapace F, Arnold MO, Rouleau JL, Pfeffer MA, Lee RT, and Solomon SD. Regional wall stress predicts ventricular remodeling after anteroseptal myocardial infarction in the Healing and Early Afterload Reducing Trial (HEART): an echocardiography-based structural analysis. Ame Heart J 2001; 141: 234–242

4. Amber D. Moelker, Timo Baks, E.J. van den Bos, R.J. van Geuns, P.J. de Feyter, Dirk J. Duncker, and W.J. van der Giessen. Reduction in infarct size, but no functional improvement after bone marrow cell administration in a porcine model of reperfused myocardial infarction. Eur Heart J 2006; 27: 3057–3064

5. Asahara T, Masuda H, Takahashi T et al. Bone marrow origin of endothelial progenitor cells responsible for postnatal vasculogenesis in physiology and pathological neovasularization. Circ Res 1999; 85: 221-228

6. Ashizawa N, Graf K, Do YS, Nunohiro T, Giachelli CM, Meehan WP, Tuan TL, Hsueh WA. Osteopontin is produced by rat cardiac fibroblasts and mediates A (II)-induced DNA synthesis and collagen gel contraction. J Clin Invest 1996; 98: 2218–2227

7. Assmus B, Schachinger V, Teupe C, Britten M, Lehmann R, Dobert N, Grunwald F, Aicher A, Urbich C, Martin H, Hoelzer D, Dimmeler S, Zeiher AM. Transplantation of progenitor cells and regeneration enhancement in acute myocardial infarction (TOPCARE-AMI). Circulation 2002; 106: 3009 –3017

8. Balsam LB, Wagers AJ, Christensen JL, Kofidis T, Weissman IL, Robbins RC. Haematopoietic stem cells adopt mature haematopoietic fates in ischemic myocardium. Nat Med 2004; 428: 668–73

9. Barbash IM, Chouraqui P, Baron J, Feinberg MS, Etzion S, Tessone A, Miller L, Guetta E, Zipori D, Kedes LH, Kloner RA, Leor J. Systemic delivery of bone marrow-derived mesenchymal stem cells to the infarcted myocardium: feasibility, cell migration, and body distribution. Circulation 2003; 108: 863–8

10. Breitbach M, Bostani T, Roell W, Xia Y, Dewald O, Nygren JM, Fries JW, Tiemann K, Bohlen H, Hescheler J, Welz A, Bloch W, Jacobsen SE, Fleischmann BK. Potential risks of bone marrow cell transplantation into infarcted hearts. Blood 2007; 110(4): 1362-1369

11. Nardi NB and Meirelles LDS. Mesenchymal stem cells: Isolation, in vitro expansion and characterization. In. Handb Exp Pharmacol 2006; 174: 249– 282

12. Campbell SE, Katwa LC: Angiotensin II stimulated expression of transforming growth factor-beta1 in cardiac fibroblasts and myofibroblasts. J Mol Cell Cardiol 1997; 29: 1947–1958

13. Chen J, Zhang Z, Li Y, Wang L, Xu Y Z, Gautam S C, Lu M, Zhu Z. Chopp M. Intravenous administration of human bone marrow stromal cells induces angiogenesis in the ischemic boundary zone after stroke in rats. Circ Res 2003; 92: 692–699

14. Chen J, Li Y, Wang L, Zhang Z, Lu D, Lu M, Chopp M. Therapeutic benefit of intravenous administration of bone marrow stromal cells after cerebral ischemia in rats. Stroke 2001; 32: 1005–1011

15. Liang C S, Wu-wang F, Jun Q, Fei Y, Yu-hao L, Shou-jie S, Jun-jie Z, Song L, Lain-ming L, Zhao R C H. Improvement of cardiac function after intracoronary transplantation of autologous bone marrow mesenchymal stem cell in patients with acute myocardial infarction. Chinese Med J 2004;117: 1443–1448

16. Chien KR: Genes and physiology: molecular physiology in genetically engineered animals. J Clin Invest 1996; 97: 901–909

17. Cleutjens JP, Verluyten MJ, Smiths JF, Daemen MJ, collagen remodeling after muocardial infarction in the rat heart. Ame J Pathol1995; 147: 325-338

18. Darby I, Skalli O, Gabbiani G. A-smooth muscle actin is transiently expressed by myofibroblasts during experimental wound healing. Lab Invest 1990; 63: 21-29

19. Denhardt DT, Guo X. Osteopontin: a protein with diverse functions. J Fed Ame Soci Exp Biol 1993; 7: 1475–1482

20. Desmouliere A, Geinoz A, Gabbiani F, Gabbiani G: Transforminutesg growth factor 1 induces smooth muscle actin expression in granulation tissue myofibroblasts and in quiescent and growing cultured fibroblasts. J Cell Biol 1993; 122: 103–111

21. Dewald O, Ren G, Duerr GD, Zoerlein M, Klemm C, Gersch C, Tincey S, Michael LH, Entman ML, Frangogiannis NG: Of mice and dogs: species specific differences in the inflammatory response following myocardial infarction. Ame J Pathol 2004; 164: 665–677

22. Dewald O, Pawel Z, Winkelmann K, Koerting A, Ren G, Abou-khamis T, Micheal L.H Rollins B.J, Entman M.L and Frangogiannis N.G. CCL2/Monocyte chemoattracent protein-1 regulates inflammatory responses critical healing myocardial infarcts. Circ Res 2005; 96: 881-889

23. Dörge H, Schulz R, Belosjorow S, Post H, van de Sand A, Konietzka I, Frede S, Hartung T, Vinten-Johansen J, Youker KA, Entman ML, Erbel R, Heusch G. Coronary microembolization, the role of TNFα_ in contractile dysfunction. J Mol Cell Cardiol 2002; 34: 51–62

24. Ducharme A, Frantz S, Aikawa M, Rabkin E, Lindsey M, Rohde LE, Schoen FJ, KellyRA, Werb Z, Libby P, Lee RT. Targeted deletion of matrix metalloproteinase-9 attenuates left ventricular enlargement and collagen accumulation after experimental myocardial infarction. J Clin Invest 2000; 106: 55-62

25. Frangogiannis NG, Youker K , Entman ML. The role of neutrophil in myocardial ischemia and reperfusion. EXS 1996; 76: 263-284

26. Frangogiannis, N. G., M. L. Lindsey, L. H. Michael, K. A.Youker, R. B. Bressler, L. H. Mendoza, R. N. Spengler, C.W.Smith, and M. L. Entman. Resident cardiac mast cells degranulate and release preformed TNF-a initiating the cytokine cascade in myocardial ischemia/reperfusion. Circulation 1998; 98: 699–710

27. Frangogiannis NG. Chemokines in the ischemic myocardium: from inflammation to fibrosis. Inflamm Res 2004; 53: 585–595

28. Frangogiannis NG, Mendoza LH, Smith CW, Michael LH, Entman. Induction of the synthesis of the C-X-C chemokine interferon-gamma-inducible protein-10 in experimental canine endotoxemia. Cell Tissue Res 2000; 302: 365–376

29. Frangogiannis,N.G, Shimoni S, Chang SM, Ren G, Shan K , Aggeli C, Reardon MJ, Letsou GV, Espada R, Ramchandani M, Mark Entman, ML. Zoghb WA. Evidence for an active inflammatory process in the hibernating human myocardium. Ame J pathol 2002; 160:1425-1433

30. Franz WM, Mueller OJ, Hartong R, Frey N, Katus HA: Transgenic animal models: new avenues in cardiovascular physiology. J Mol Med 1997; 75: 115-129

31. Ford ES, Giles WH, Dietz WH (2002). Prevalence of metabolic syndrome among US adults: findings from the third National Health and Nutrition Examination Survey. JAMA 2002; 287(3): 356-359

32. Gerdes AM, Capasso JM. Structural remodeling and mechanical dysfunction of cardiac myocytes in heart failure. J Mol Cell Cardiol 1995; 27: 849–856

33. Giachelli CM, Schwartz SM, Liaw L. Molecular and cellular biology of Osteopontin: potential role in cardiovascular disease. Trends Cardiovasc Med 1995; 5 88-:95

34. Gurevitch J, Frolkis I, Yuhas Y, Paz Y, Matsa M, Mohr R, Yakirevich V Tumor necrosis factor-alpha is released from the isolated heart undergoing ischemia and reperfusion. J Ame Coll Cardiol 1996; 28: 247–252

35. Hayashidani S, Tsutsui H, Shiomi T, Ikeuchi M, Matsusaka H, Suematsu N, Wen J, Egashira K, Takeshita A. Anti-monocyte Chemoattractant protein-1 gene therapy attenuates left ventricular remodeling and failure after experimental myocardial infarction. Circulation 2003; 108: 2134–2140

36. Hou D, Youssef EA, Brinton TJ, Zhang P, Rogers P, Price ET, Yeung AC, Johnstone BH, Yock PG, March KL. Radiolabeled cell distribution after intramyocardial, intracoronary, and interstitial retrograde coronary venous delivery: implications for current clinical trials. Circulation 2005; 112: I150– 1156

37. Hwang MW, Matsumori A, Furukawa Y, Ono K, Okada M, Iwasaki A, Hara M, Miyamoto T, Touma M, Sasayama S: Neutralization of interleukin- 1beta in the acute phase of myocardial infarction promotes the progression of left ventricular remodeling. J Ame Coll Cardiol 2001; 38:1546–1553

38. Irwin MW, Mak S, Mann DL, Qu R, Penninger JM, Yan A, Dawood F, Wen W-H, Shou Z, Liu P. Tissue expression and immunolocalization of tumor necrosis factor in post infarction dysfunctional myocardium. Circulation 1999; 99: 1492–1498

39. Jackson BM, Gorman JH, Moainie SL, Guy TS, Narula N, Narula J, John-Sutton MG, Edmunds LH, Jr., Gorman RC. Extension of border zone myocardium in postinfarction dilated cardiomyopathy. J Ame Coll Cardiol 2002; 40: 1160 –1167

40. Jackson BM, Parish LM, Gorman JH, III, Enomoto Y, Sakamoto H, Plappert T, St John Sutton MG, Salgo I, Gorman RC. Borderzone geometry after acute myocardial infarction: A three-dimensional contrast enhanced echocardiographic study. Ann Thorac Surg 2005; 80: 2250 –2255

41. James JF, Hewett TE, Robbins J: Cardiac physiology in transgenic mice. Circ Res 1998; 82:407-415

42. Jugdutt BI, Hutchins GM, Bulkley BH, Becker LC: Myocardial infarction in the conscious dog: three-dimensional mapping of infarct, collateral flow and region at risk. Circulation 1976; 60: 1141-1150

43. Kaartinen MT, Pirhonen A, Linnala-Kankkunen A, Maenpaa PH. Crosslinking of osteopontin by tissue transglutaminutesase increases its collagen binding properties. J Biol Chem 1999; 274: 1729–1735

44. Kaikita K, Hayasaki T, Okuma T, Kuziel WA, Ogawa H, Takeya M. Targeted deletion of CC chemokine receptor 2 attenuates left ventricular remodeling after experimental myocardial infarction. Ame J Pathol 2004; 165: 439–447

45. Kapadia S, Oral H, Lee J, Taffet G, Mann DL .Hemodynamic regulation of tumor necrosis factor alpha-gene and protein expression in adult feline myocardium, 1997

46. Katwa LC: Cardiac myofibroblasts isolated from the site of myocardial infarction express endothelin de novo. Ame J Physiol 2003, 285: H1132–H1139

47. Kawamoto A, Gwon HC, Iwaguro H, Yamaguchi J, Uchida S, Masuda H, Silver M, Ma H, Kearney M, Isner JM, Asahara T. Therapeutic potential of ex vivo expanded endothelial progenitor cells for myocardial ischemia. Circulation 2001; 103: 634–637

48. Kersten JR, pagel Ps, chilian WM. Warltier DC.multifactorial basis for coronary collateralization: a complex adapative response to ischemia. Cardiovasc Res 1999; 43: 44-57

49. Lunde K, Solheim S , Aakhus S, Arnesen H, Abdelnoor M, Egeland T, Endresen K, Ilebekk A, Mangschau A, Fjeld JG, Smith HJ, Taraldsrud E, Grogaard HK, Bjornerheim R, Brekke M, Muller C, Hopp E, Ragnarsson A, Brinchmann JE, Forfang K. N Eng J Med 2006; 355: 1199-1209

50. Kim JS, et al. Expression of monocyte chemoattractant protein-1 and macrophage inflammatory protein-1 after focal cerebral ischemia in the rat. J Neuroimm 1995; 56: 127–134

51. Kocher AA, Schuster MD, Szabolcs MJ, Takuma S, Burkhoff D, Wang J, Homma S, Edwards NM, and Itescu S. Neovascularization of ischemic myocardium by human bone marrow-derived endothelial precursors prevents post-infarction remodeling and improves cardiac function. Nat Med 2001; 7: 430–436

52. Kolossov E, Bostani T, Roell W, Breitbach M, Pillekamp F, Nygren JM, Sasse P, Rubenchik O, Fries JW, Wenzel D, Geisen C, Xia Y, Lu Z, Duan Y, Kettenhofen R, Jovinge S, Bloch W, Bohlen H, Welz A, Hescheler J, Jacobsen SE, Fleischmann BK. Engraftment of engineered ES cell-derived cardiomyocytes but not BM cells restores contractile function to the infarcted myocardium. J Exp Med 2006; 203: 2315-23 27

53. Kudo M, Wang Y, Wani M, Ayub A, Ashraf M. Implantation of bone marrow reduces the infarction and fibrosis in ischemic mouse heart. J Mol Cell Cardiol 2003; 35: 1113–1119

54. Kurrelmeyer KM, Michael LH, Baumgarten G,Taffet GE, Peschon JJ, Sivasubramanian N, Entman ML, Mann DL. Endogenous tumor necrosis factor protects the adult cardiac myocyte against ischemic- induced apoptosis in a murine model of acute myocardial infarction. Proc Natl Academic Science USA 2000; 97: 5456-5461

55. Lacraz S, Nicod LP, Chicheportiche R, Welgus HG, Dayer JM. IL-10 inhibits metalloproteinase and stimulates TIMP-1 production in human mononuuclear phagocytes. J Clin Invest 1995; 2304-231

56. Laflamme MA, Myerson D, Saffitz JE, et al. Evidence for cardiomyocyte repopulation by extracardiac progenitors in transplanted human hearts. Circ Res 2002; 90: 634–640

57. Lefer AM, Tsao P, Aoki N, Palladino MA Jr: Mediation of cardioprotection by transforming growth factor-beta. Science 1990; 249: 61–64

58. Lu L, Smith ZG, Woessner JF, Ursell PC, Nissen T, Galardy RE, Xu Y, Zhu P,and Schwartz GG. Matrix metalloproteinases and collagen ultrastructure in moderate myocardial ischemia and reperfusion in vivo. Am J Physiol, Heart Circ Physiol 2000; 279 : H601–H609

59. Lutgens E, Daemen MJ, de Muinck ED, Debets J, Leenders P, Smits JF. Chronic myocardial infarction in the mouse: cardiac structural and functional changes. Cardiovasc Res 1999; 41: 586–593

60. Marcin Bujak and Nikolaos G Frangogiannis. The role of TGF-β Signaling in Myocardial Infarction and Cardiac Remodeling. Cardiovasc Res 2007; 74(2): 184–195

61. Martire A, Fernandez B, Buehler A, Strohm C, Schaper J, Zimmermann R, Kolattukudy PE, Schaper W. Cardiac overexpression of monocyte chemoattractant protein-1 in transgenic mice mimics ischemic preconditioning through SAPK/JNK1/2 activation. Cardiovasc Res 2003; 57: 523–534

62. Masaki Ikeuchi, Hiroyuki Tsutsui , Tetsuya Shiomi, Hidenori Matsusaka, Shouji Matsushima, Jing Wen, Toru Kubota, Akira Takeshita. Inhibition of TGF- signaling exacerbates early cardiac dysfunction but prevents late remodeling after infarction. Cardiovasc Res 2004; 64: 526–535

63. Mehta JL, LI DY .inflammation in ischemic heart disease: response to tissue injury or a pathologentic villain cardiovascular Research 1999; 43: 291-299

64. Michael LH, Lewis RM, Brandon TA, Entman ML: Cardiac lymph flow in conscious dogs. Ame J Physiol 1979; 237: H311–317

65. Mossmann TR. Properties and functions of interleukin- 10. Advan Immun 1994; 56: 1-22

66. Muller P, Pfeiffer P, Koglin J, et al. Cardiomyocytes of noncardiac origin in myocardial biopsies of human transplanted hearts. Circulation 2002; 106: 31–35

67. Mukherjee BB, Nemir M, Beninati S, Cordella-Miele E, Singh K, Chackalaparampil I, Shanmugam V, DeVouge MW, Mukherjee AB. Interactionof osteopontin with fibronectin and other extracellular matrix molecules. Ann N Y Academic Science 1995; 760: 201–212

68. Murry CE, Field LJ, Menasche P. Cell-based cardiac repair: reflections at the 10-year point. Circulation 2005; 112: 3174-3183

69. Murry CE, Giachelli CM, Schwartz SM, Vracko R. Macrophages express osteopontin during repair of myocardial necrosis. Ame J Pathol 1994; 145: 1450–1462

70. Murry CE, Soonpaa MH, Reinecke H, Nakajima H, Nakajima HO, , Rubart M, Pasumarthi KBS, Virag JI, Bartelmez SH, Poppa V, Bradford G, Dowell JD, Williams DA and Field LJ. Haematopoietic stem cells do not transdifferentiate into cardiac myocytes in myocardial infarcts. Nature 2004; 428: 664- 668

.

71. MP Boyle and HF Weisman**.** Limitation of infarct expansion and ventricular remodeling by late reperfusion. Study of time course and mechanism in a rat model. Circulation 1993; 88: 2872-2883

72. Nossuli TO, Lakshminutesarayanan V, Baumgarten G, Taffet GE, Ballantyne CM, Michael LH, Entman ML: A chronic mouse model of myocardial ischemia-reperfusion: essential in cytokine studies. Ame J Physiol Heart Circ Physiol 2000; 278: 1049-1055

73. Nygren JM, Jovinge S, Breitbach M et al. Bone marrow-derived hematopoietic cells generate cardiomyocytes at a low frequency through cell fusion, but not transdifferentiation. Nat Med 2004; 10: 494-501

74. Olivetti G, Capasso JM, Sonnenblick EH, Anversa P. Side-to-side slippage of myocytes participates in ventricular wall remodeling acutely after myocardial infarction in rats. Circ Res 1990; 67: 23–34

75. Ono K, Matsumori A, Shioi T, Furukawa Y, Sasayama S .Cytokine gene expression after myocardial infarction in rat hearts. Circulation 1998; 98: 149–156

76. Orlic D, Kajstura J, Chimenti S, Jakoniuk I, Anderson SM, Li B, Pickel J, McKay R, Nadal-Ginard B, Bodine DM, Leri A, and Anversa P. Bone marrow cells regenerate infarcted myocardium. Nature 2001; 410: 701–705

77. Orlic D. Stem cell repair in ischemic heart disease: an experimental model. Int J Hematol 2002; 76 : 144-145

78. Ophascharoensuk V, Giachelli CM, Gordon K, Hughes J, Pichler R, Brown P, Liaw L, Schmidt R, Shankland SJ, Alpers CE, Couser WG and Johnso RJ. Obstructive uropathy in the mouse: role of osteopontin in interstitial fibrosis and apoptosis. Kidney International 1999; 56: 571–580

79. Pfeffer MA, Braunwald E. Ventricular remodeling after myocardial infarction. Experimental observations and clinical implications. Circulation 1990; 81: 1161–1172

80. Pfeffer MA, Pfeffer JM, Fishbein MC, Fletcher PJ, Spadaro J, Kloner RA, Braunwald E. Myocardial infarct size and ventricular function in rats. Circ Res 1979; 44: 503–512

81. Persy VP, Verstrepen WA, Ysebaert DK, Greef KED and Bore MED. Differences in osteopontin up-regulation between proximal and distal tubules after renal

82. Peterson JT, Li H, Dillon L, Bryant JW. Evolution of matrix metalloprotease and tissue inhibitor expression during heart failure progression in the infarcted rat. Cardiovasc Res 2000; 46: 307–315

83. Reinecke, H., Poppa, V. and Murry, C. E. Skeletal muscle stem cells do not transdifferentiate into cardiomyocytes after cardiac grafting. J Mol Cell Cardiol 2002; 34: 241-249

84. Richard, V., C. E. Murry, and K. A. Reimer. Healing of myocardial infarcts in dogs: effects of late reperfusion. Circulation 1995; 92: 1891–1901

85. Robert A. Kloner, Roberto Bolli, Eduardo Marban, Leslie Reinlib, Eugene Braunwald, and Participants. Medical and Cellular Implications of Stunning, Hibernation, and Preconditioning An NHLBI Workshop. Circulation. 1998; 97: 1848-1867

86. Roell W, Lu ZJ, Bloch W, Siedner S, Tiemann K, Xia Y, Stoecker E, Fleischmann M, Bohlen H, Stehle R, Kolossov E, Brem G, Addicks K Pfitzer G, Welz A, Hescheler J, and Fleischmann BK. Cellular cardiomyoplasty improves survival after myocardial injury. Circulation 2002; 105: 2435–2441

87. Rohde LE, Ducharme A, Arroyo LH, Aikawa M, Sukhova GH, Lopez –Anaya A, et al. Matrix metalloproteinase inhabitation attenuates early left ventricular enlargement after experimental myocardial infarction in mice. Circulation 1999; 99(23): 3063-70

88. Rosamond W, Flegal K, Friday G, Furie K, Go A, Greenlund K, Haase N, Ho M, Howard V, Kissela B, Kittner S, Lloyd-Jones D, McDermott M, Meigs J, Moy C, Nichol G, O'Donnell CJ, Roger V, Rumsfeld J, Sorlie P, Steinberger J, Thom T, Wasserthiel-Smoller S, Hong Y, for the American Heart Association Statistics Committee and Stroke Statistics Subcommittee. Heart disease and stroke statistics: 2007 update: a report from the American Heart Association Statistics Committee and Stroke Statistics Subcommittee. Circulation 2007; 115: e69–e171

89. Sam F, Sawyer DB, Chang DL, Eberli FR, Ngoy S, Jain M, Aminutes J, Apstein CS, Colucci WS. Progressive left ventricular remodeling andapoptosis late after myocardial infarction in mouse heart. Ame J Physiol 2000; 279: H422–H428

90. Salcedo R, Ponce ML, Young HA, Wasserman K, Ward JM, Kleinman HK, Oppenheim JJ, Murphy WJ. Human endothelial cells express CCR2 and respond to MCP-1: direct role of MCP-1 in angiogenesis and tumor progression. Blood 2000; 96: 34–40

91. Sakakibara Y, Tambara K, Lu F, Nishina T, Nagaya N, Nishimura K, and Komeda M. Cardiomyocyte transplantation does not reverse cardiac remodeling in rats with chronic myocardial infarction. Ann Thorac Surg 2002; 74: 25–30

92. Schachinger V, Assmus B, Britten MB,Honold J, Lehmann R, Teup C, Abolmaali ND, Vogl TJ, Hofmann WK, Martin H, Dimmeler S and Zeiher AM. Transplantation of progenitor cells and regeneration enhancement in acute myocardial infarction: final one-year results of the TOPCARE-AMI Trial. J Ame Coll Cardiol 2004; 44: 1690–1699

93. Schaper W, Ito Wd. Molecular mechanisms of coronary collateral vessel growth. Circ Res 1996; 79: 911-919

94. Shah M, Foreman DM, Ferguson MW: Neutralisation of TGF-β_1 and TGF-β_2 or exogenous addition of TGF-β_3 to cutaneous rat wounds reduces scarring. J Cell Sci 1995; 108: 985–1002

95. Shah M, Foreman DM, Ferguson MW: Neutralising antibody to TGF-β1, 2 reduces cutaneous scarring in adult rodents. J Cell Sci 1994; 107: 1137–1157

96. Strauer BE, Brehm M, Zeus T, Kostering M, Hernandez A, Sorg RV, Kogler G, Wernet P. Repair of infarcted myocardium by autologous intracoronary mononuclear bone marrow cell transplantation in humans. Circulation 2002; 106: 1913 – 8

97. Suzuki K, Murtuza B, Smolenski RT, Sammut IA, Suzuki N, Kaneda Y,Yacoub MH: Over expression of interleukin-1 receptor antagonist provides cardioprotection against ischemia-reperfusion injury associated with reduction in apoptosis. Circulation 2001; 104: I308–I313

98. Tanaka.Y., D.H. Adams, S. Hubscher, H. Hirano, U. Siebenlist, and S. Shaw. T-cell adhesion induced by proteoglycan immobilized cytokine MIP-1B. Nature 1993; 361: 79-82

99. Tarzami ST, Cheng R, Miao W, Kitsis RN, Berman JW. Chemokine expression in myocardial ischemia: MIP-2 dependent MCP-1 expression protects cardiomyocytes from cell death. J Mol Cell Cardiol 2002; 34: 209–221

100. Thielmann M, Dörge H, Martin C, Belosjorow S, Schwanke U, van de Sand A, Konietzka I, Büchert A, Krüger A, Schulz R, Heusch G .Myocardial dysfunction with coronary microembolization: signal transduction through asequence of nitric oxide, tumor necrosis factor and sphingosine. Circ Res 2002; 90: 807–813

101. Tomasek JJ, Gabbiani G, Hinz B, Chaponnier C and Brown RA. Myofibroblasts and mechano-regulation of connective tissue remodeling. Nat Rev Mol Cell Biol 2002; 3: 349-363

102. Tomita S, Mickle DA, Weisel RD, Jia ZQ, Tumiati LC, Allidina Y, Liu P and Li RK. Improved heart function with myogenesis and angiogenesis after autologous porcine bone marrow stromal cell transplantation. J Thorac Cardiovasc Surg 2002; 123: 1132-1140

103. Wang T, Tang W, Sun S, Ristagno G, Huang Z and Weil MH, Intravenous infusion of bone marrow mesenchymal stem cells improves myocardial function in a rat model of myocardial ischemia .Crit Care Medicine 2008; 36: 486-491

104. Van Kerckhoven R, Kalkman EA, Saxena PR, Schoemaker RG. Altered cardiac collagen and associated changes in diastolic function of infarcted rat hearts. Cardiovasc Res 2002; 46: 316–323

105. Virag JI, Murry CE. Myofibroblast and endothelial cell proliferation during murine myocardial infarct repair. Ame J Pathol 2003; 163: 2433–2440

106. Willems IE ,. Havenith M. G, De Mey J. G., and Daemen M. J. The alpha-smooth muscle actin-positive cells in healing human myocardial scars. Ame J Pathol 1994; 145(4): 868–875

107. Wollert KC, Meyer GP, Lotz J, et al. Intracoronary autologous bone marrow cell transfer after myocardial infarction: the BOOST randomised controlled clinical trial. Lancet 2004; 364:141

108. Weber KT, Sun Y, Tyagi SC, Cleutjens JP. Collagen network of the myocardium: function, structural remodeling and regulatory mechanisms. J Mol Cell Cardiol 1994; 26: 279–292

109. Yang F, Liu YH, Yang XP, Xu J, Kapke A, Carretero OA. Myocardial infarction and cardiac remodeling in mice. Exp Physiol 2002; 87: 547–555

7 Acknowledgements

First and the foremost, I would like to express my special gratitude to my supervisors Prof. Dr.med. B. K. Fleischmann and Priv. - Doz. Dr. med. O. Dewald for their whole cordial support that they conferred throughout my stay in the laboratory. I thank Prof. Dr. med. Fleischmann for giving me the opportunity to carry out my research in his laboratory and for his helpful comments and support all the way through.

Priv. - Doz. Dr. med. Dewald had been extremely instrumental in shaping every aspect of my practical part of the thesis and without his keen interest, remarkable scientific expertise and his friendly supervision on my thesis would not have seen this day of light. I feel proud and privileged to have him as my adviser.

I would like to thank Miss Christine Peigney for her help with staining and cutting the section and for her warm and friendly discussions which I had with her during this time.

During my stay in Life & Brain laboratory, I came in contact with several fascinating people with whom I shared great companionship.

Many thanks to my colleagues in heart surgery laboratory for creating a great atmosphere and good team work over the years. I would like to express my special thanks to Dr. Daniel Dürr for critically reviewing my results and for his support at many levels throughout my work. I am also grateful to Priv. - Doz. Dr. med. W. Roell and Dr. rer. nat. M. Breitbach. Last but certainly not the least; I would like to let my family know how much they mean to me and that without their support and encouragement I would not have come that far. I am especially thankful to my husband Gumua Tarhuni for his continuous support and keeping up my spirits in difficult situations. I am greatly indebted to them for which I can never thank them enough.